

CATEGORIFICATION OF SOME PENROSE POLYNOMIALS

DANIEL W. COLLISON AND DANIEL TUBBENHAUER

ABSTRACT. We construct doubly- and triply-graded Penrose-type homologies for ribbon graphs. The construction is a TQFT-valued cube of resolutions built from two-dimensional cobordisms, which may be nonorientable. Their Euler characteristics recover specializations of some Penrose polynomials; in particular, the four color case comes with a refinement of the classical Penrose criterion.

CONTENTS

1. Introduction	1
2. Möbius TQFTs	4
3. Graph invariants	7
4. Möbius Frobenius algebras	18
5. A choice related to n -coloring	20
6. Examples and computer talk	24
References	32

1. INTRODUCTION

In this paper, we categorify some Penrose polynomials.

1A. Some history. The Penrose polynomial is one of the classical meeting points of graph coloring, topology, and diagrammatics. Its origin is Penrose’s graphical calculus for tensor webs [Pen71], which detects Tait colorings in the planar trivalent case: the evaluation at 3 counts proper 3-edge colorings, or equivalently, 4-face colorings after planar duality. Thus the Penrose polynomial is closely tied to the four color theorem, but in a local, diagrammatic form. Aigner developed the corresponding Penrose polynomial for plane graphs [Aig97], which Ellis-Monaghan–Moffatt later extended to embedded graphs and related to twisted duality, transition polynomials, and ribbon-graph structure [EMM13]; see also [EKM18] for a useful account of how Penrose’s coloring calculus fits into the world of topological graph polynomials.

The feature that makes the Penrose polynomial so adaptable is that it is a local state sum. Similarly to lattice models in statistical mechanics, the construction involves resolving local pieces, attaching weights, and summing over the resulting states. The resulting polynomial is thus closely related to Jaeger’s transition polynomial [Jae90] and the topological transition polynomial viewpoint for ribbon graphs, as well as the Bollobás–Riordan polynomial, one of the basic extensions of the Tutte polynomial to graphs on surfaces [BR02], and also Chmutov’s partial-duality framework [Chm09]; in all these instances, graph polynomials are not isolated gadgets: they are different shadows of local operations on embedded graphs.

The second relevant history is homological. Khovanov homology showed that a local state sum can be the Euler characteristic of a more refined invariant [Kho00] (such a refinement is often called categorification), and Bar-Natan’s formulation made the underlying (1+1 or 2D) TQFT structure explicit [BN05]. Soon after, similar ideas were applied to graph polynomials: for example, Helme-Guizon–Rong categorified the chromatic polynomial [HGR05], Jasso-Hernandez–Rong categorified a version of the Tutte polynomial [JR06], and Loeb1–Moffatt categorified the chromatic polynomial of fatgraphs and the Bollobás–Riordan polynomial [LM08], to name a few; while not technically used below, these papers explain the guiding philosophy: a cube of local resolutions can remember more than its Euler characteristic.

Mathematics Subject Classification 2020. Primary: 05C31, 57R56; Secondary: 05C15, 57K18, 57M15.

Keywords. Penrose polynomial, graph coloring, four color theorem, topological quantum field theories, categorification, nonorientable cobordisms.

The closest relatives of the present paper come from two directions. The first direction is the graph coloring homology story built from perfect matchings and TQFTs. Baldridge constructed a cohomology theory for planar trivalent graphs equipped with a perfect matching; its graded Euler characteristic is the 2-factor polynomial [Bal18]. Baldridge–McCarty then presented an unoriented TQFT interpretation of the Penrose polynomial in which filtered homology counts face colorings of ribbon graphs [BM23]. The second direction is virtual link homology. There is a specific “funny face” that appears in the cube of resolutions, which can be dealt with in a natural way by introducing nonorientability into Bar-Natan’s cobordism picture; see e.g. [Man07, Tag13, Tub14]. Both perspectives are important for us: perfect matchings give the cube, and nonorientable cobordisms provide the extra local map.

The present paper makes use of the above ideas, with the crucial difference being that we use a different local ingredient.

Remark 1A.1. There is also a representation-theoretic reading of the above story. Already Penrose’s original graphical calculus is a tensor calculus: trivalent vertices represent invariant tensors and edges represent contractions; in the planar trivalent case, this is closely related to the \mathfrak{so}_3 weight-system evaluation (or equivalently, SO_3 -webs), which is called even Temperley–Lieb or even Verlinde calculus. Using the same language, Tait colorings and the four color theorem can be reformulated in representation-theoretic terms; see e.g. [BN97, MPS17, TL71, Tub24a, Yam89], and for categorified versions of this viewpoint using foams and gauge theory, see e.g. [KR21, KM19]. \diamond

1B. This paper’s contribution. We work with trivalent ribbon graphs equipped with a perfect matching.

Remark 1B.1. We will see in Section 3A that this is not a restriction. \diamond

Resolving the matching edges produces a cube of states. As usual, an edge of the cube can either merge two circles or split one circle into two. In our setting, there is a third possibility: one circle stays one circle, but the local surface contribution is nonorientable. Algebraically, the first two moves are controlled by the multiplication and comultiplication of a Frobenius algebra respectively, while the third move is controlled by one extra endomorphism.

Before introducing the formal terminology, the algebraic input can therefore be summarized as follows: take a commutative Frobenius algebra V , with multiplication μ and comultiplication Δ , together with an endomorphism $m: V \rightarrow V$. The compatibility relations dictate that m can be moved through multiplication, and that

$$(1B.2) \quad m^2 = \mu \circ \Delta,$$

which is a key relation required for the new square faces in the cube to commute. The usual sign assignment then turns the cube into a chain complex. In slogan form,

A Penrose-type state sum can be lifted to a homology theory by allowing one nonorientable local map.

The corresponding nonorientable TQFTs (called Möbius TQFTs or MTQFTs), together with the associated Frobenius algebras (called Möbius Frobenius algebras), are introduced later in Section 2 and Section 4. The construction itself is the important point: a cube of resolutions with three local maps, μ, Δ, m .

Our main result is that the resulting homology is an invariant of perfect matching ribbon graphs. Its graded Euler characteristic is the bracket defined by the local relations in Definition 3B.1, repeated here without further explanation:

$$\begin{aligned} \langle \text{diagram} \rangle &= A \langle \text{diagram} \rangle + B \langle \text{diagram} \rangle, \\ \langle \text{diagram} \rangle &= C, \\ \langle \Gamma_1 \sqcup \Gamma_2 \rangle &= \langle \Gamma_1 \rangle \cdot \langle \Gamma_2 \rangle, \end{aligned}$$

with

$$A = 1, \quad B = -q_1^{s_1} \cdots q_m^{s_m}, \quad C = q \dim(V),$$

where $q\dim$ is the graded dimension, and the q_i are grading variables. As usual, the bracket is the shadow of the homology.

We then construct an explicit family of examples. Given an integer $n > 0$, set

$$(1B.3) \quad V_n = \mathbb{Z}[\frac{1}{3n}][x, y]/(x^n, y^3 - xy).$$

A suitable Frobenius trace, together with a suitable choice of endomorphism m , gives the required algebraic input. The grading is by $\mathbb{Z}/n\mathbb{Z} \times \mathbb{Z}/2\mathbb{Z}$ for n even, and by $\mathbb{Z}/n\mathbb{Z}$ for n odd, plus, in both cases, a \mathbb{Z} -grading from the homology. The homology is therefore either doubly- or triply-graded, depending on the parity of n .

Remark 1B.4. The algebra $\mathbb{C}[x, y]/(x^n, y^3 - xy)$ has a nice topological model. Suppose that x and y have degree 4 and 2 respectively, and let \mathbb{H} denote quaternions. Let η be the tautological quaternionic line bundle over $\mathbb{H}\mathbb{P}^{n-1}$, viewed as a complex rank two bundle, and consider the complex projective bundle

$$\mathbb{P}(\eta \oplus \mathbb{C}) \longrightarrow \mathbb{H}\mathbb{P}^{n-1}.$$

By the projective bundle formula,

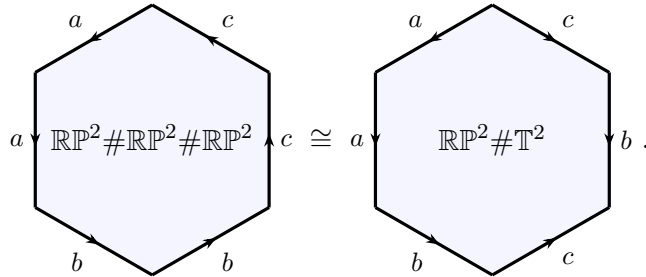
$$H^*(\mathbb{P}(\eta \oplus \mathbb{C}); \mathbb{C}) \cong \mathbb{C}[x, y]/(x^n, y^3 - xy),$$

up to the harmless sign convention. The algebra used in this paper can therefore be viewed as a quaternionic analog of the familiar Frobenius algebra $\mathbb{C}[x]/(x^n) \cong H^*(\mathbb{C}\mathbb{P}^{n-1}; \mathbb{C})$ that is crucial to the construction of link homologies. \diamond

The corresponding Euler characteristic recovers specializations of the Penrose polynomial $P(\Gamma, n)$: for n even, two specializations give $P(\Gamma, 3n)$ and $P(\Gamma, n)$, while for n odd one obtains $P(\Gamma, 3n)$. In particular, the case $n = 4$ produces a homological refinement of the Penrose polynomial test for four face colorability.

Remark 1B.5. The $\mathbb{Z}/2\mathbb{Z}$ -grading is genuinely new as far as we can tell, and it appears in the case relevant to the four color theorem; this gives a new graded refinement of the classical Penrose polynomial criterion for four face colorability: instead of asking only for a nonzero number at the end, one can ask for a stronger positivity statement before collapsing the grading. In this sense, the extra grading suggests a new homological route toward the four color theorem.

It is also not a formal accident, which is remarkable in itself. As we will see, the grading is tied to the nonorientable part of the construction, and it is essentially controlled by the Dyck surface, and Dyck's theorem, which is (in polygon notation of surfaces):



As we will see, another way of saying this is that we use the monoid structure of our MTQFT. \diamond

The homology is stronger than its Euler characteristic, as expected, and we show this already on small examples: two nonisomorphic perfect matching graphs can have the same bracket but different homology; even more surprising, the bracket may vanish while the homology does not, cf. [Section 6](#). In fact, for the family V_n above, we show that the homology is strictly stronger than the bracket for every positive integer n . The final section includes the accompanying computer calculations, which build the cube, insert the local maps, check that $d^2 = 0$, and compute the resulting Poincaré polynomial.

Remark 1B.6. Remarkably, there are many categorifications of the Penrose-type polynomials, which are all slightly different in nature. Let us now describe how the present construction relates to other categorifications of Penrose-type invariants. There are two nearby strands of work.

First, Luse–Rong and Kauffman give Penrose-type categorifications in the general graph-homology tradition [[LR11](#), [Kau25](#)]. The relation to our construction is as follows:

- (a) Luse–Rong categorify integer evaluations of the Penrose polynomial of a graph. Their work is close to ours in name and motivation, but their construction is not a TQFT-valued cube built from a Möbius local operation.
- (b) Kauffman’s framework is broader: it treats chromatic, dichromatic and Penrose-type data using enhanced-state constructions. In particular, triply-graded Penrose-related homologies already appear there. Our point is not merely triply gradedness, but the specific TQFT mechanism producing it.

Second, there is Baldridge–McCarty’s TQFT approach to graph coloring [BM23], which is also TQFT-based, uses unoriented/nonorientable topology, and is designed to encode face colorings of ribbon graphs. Nevertheless, the present construction is different in several concrete ways:

- (c) Baldridge–McCarty essentially use the familiar one-variable Frobenius algebra $\mathbb{C}[x]/(x^n)$, the cohomology ring of $\mathbb{C}\mathbb{P}^{n-1}$, and its filtered variant, for their theory. Our explicit family uses instead the two-variable algebra V_n of (1B.3), whose cohomological model is a projective bundle over quaternionic projective space, which is somewhat richer.
- (d) Baldridge–McCarty also have a one-circle-to-one-circle local map, but it is not the Möbius generator used here. In our construction the third local map is the Möbius endomorphism m , and the crucial square relation is (1B.2).
- (e) In the explicit family constructed below, the MTQFT mechanism produces doubly- and triply-graded homologies; in particular, the four color specialization is triply graded. They also use a shifted comultiplication in some cases to ensure that the differential preserves the grading, but we do not have this.

The novelty here is not merely that Penrose-type invariants admit homological lifts, nor merely that unoriented or nonorientable topology can be used. The new point is the specific quaternionic-enriched MTQFT lift of the Penrose-type bracket. The examples in Section 6 then show that the resulting homology retains information which is invisible to the bracket itself. \diamond

Finally, let us stress that our homology is very amenable to calculations, either by hand (using the partition-style and Deligne-type categories) or computer (code can be found in [CT26a]).

1C. Structure of the paper. The paper is organized as follows. In Section 2, we recall the relevant nonorientable two dimensional TQFTs. In Section 3, we define the Penrose-type bracket and construct the chain complex. In Section 4, we translate the construction into Frobenius-algebra-language. In Section 5, we introduce the family V_n and compare the Euler characteristic with the Penrose polynomial. Finally, in Section 6 we compute examples and discuss the code.

Acknowledgments. DT thanks Scott Baldridge for inspiring the idea behind this paper during many enjoyable discussions in Korea, and thanks the Korea Institute for Advanced Study for hosting the visit. This paper is part of the first author’s PhD thesis. DC was supported by the Commonwealth through an Australian Government Research Training Program Scholarship [https://doi.org/10.82133/C42F-K220]. DT is supported by ARC Future Fellowship FT230100489. If the reader finds parts of the construction disorienting, then at least the exposition is topologically faithful.

2. MÖBIUS TQFTS

We begin by introducing the notion of a (1+1 or 2D) *Möbius topological quantum field theory* (**MTQFT** for short). We assume the reader has some familiarity with TQFT constructions, see e.g. [Koc04] for more details.

2A. The geometric version. First recall the monoidal category **MCob**, with the nonnegative integers as objects and nonorientable two-dimensional cobordisms as morphisms (see [CT26b], which was motivated by many works such as [BKM22, BM23, Cze24, Tub14, TT06]). **MCob** has disjoint union as the monoidal product, and is symmetric, pivotal, and has a generator-relation presentation

with generators:

$$(2A.1) \quad 1_1 = \text{id}_1: \text{cylinder}, \quad \mu: \text{pants}, \quad \eta: \text{cup}, \quad \Delta: \text{pants-up}, \quad \epsilon: \text{cap}, \quad s: \text{swap},$$

together with

$$(2A.2) \quad m = \text{cylinder with lightning bolt}, \quad \text{lightning bolt} = \text{eye-shaped surface with arrows} = \mathbb{RP}^2,$$

which represents the connected sum of a cylinder and the real projective plane \mathbb{RP}^2 i.e. a Möbius strip glued to the identity cobordism [CT26b, Theorem 3.9]. The generators in (2A.1) are called cylinder (or identity), pants, cup, pants-up, cap, and swap, and m in (2A.2) is called the Möbius generator.

We list all the relations between the generators below for completeness:

$$(2A.3) \quad s^2 = 1_2,$$

$$(2A.4) \quad (1_1 \otimes s) \circ (s \otimes 1_1) \circ (1_1 \otimes s) = (s \otimes 1_1) \circ (1_1 \otimes s) \circ (s \otimes 1_1),$$

$$(2A.5) \quad s \circ (1_1 \otimes \eta) = \eta \otimes 1_1,$$

$$(2A.6) \quad (1_1 \otimes \mu) \circ (s \otimes 1_1) \circ (1_1 \otimes s) = s \circ (\mu \otimes 1_1),$$

$$(2A.7) \quad (1_1 \otimes \epsilon) \circ s = \epsilon \otimes 1_1,$$

$$(2A.8) \quad (1_1 \otimes s) \circ (s \otimes 1_1) \circ (1_1 \otimes \Delta) = (\Delta \otimes 1_1) \circ s,$$

$$(2A.9) \quad \mu \circ (1_1 \otimes \eta) = 1_1 = \mu \circ (\eta \otimes 1_1),$$

$$(2A.10) \quad (1_1 \otimes \epsilon) \circ \Delta = 1_1 = (\epsilon \otimes 1_1) \circ \Delta,$$

$$(2A.11) \quad (\mu \otimes 1_1) \circ (1_1 \otimes \Delta) = \Delta \circ \mu = (1_1 \otimes \mu) \circ (\Delta \otimes 1_1),$$

$$(2A.12) \quad \mu \circ s = \mu,$$

together with

$$(2A.13) \quad \mu \circ (m \otimes 1_1) = m \circ \mu = \mu \circ (1_1 \otimes m),$$

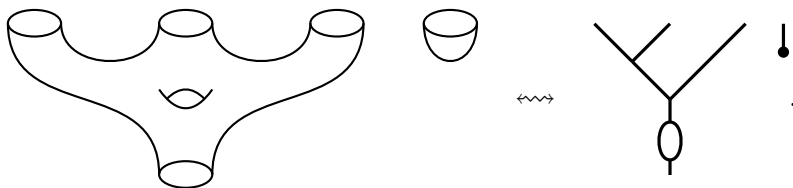
$$(2A.14) \quad s \circ (m \otimes 1_1) = (1_1 \otimes m) \circ s,$$

$$(2A.15) \quad m^3 = h \circ m,$$

where we define the handle as

$$h: \text{cylinder with cup} = \text{cylinder with pants and cup} = \mu \circ \Delta.$$

Remark 2A.16. The relations (2A.3)–(2A.12) with identical generators provide a generator-relation presentation for the (skeletal) category of oriented cobordisms $\mathbf{2Cob}$; see e.g. [Koc04]. We would recommend visualizing these before continuing. Helpful are *spine diagrams*:



(We do not know the original reference for spine diagrams, but this visual simplification is well-known.) \diamond

When working with spine diagrams, let us use a hollow dot for handles h and a filled dot for a Möbius generator m . The relations (2A.13) and (2A.14) in terms of spine diagrams are

$$\begin{array}{c} \text{---} \cdot \text{---} \\ \diagup \quad \diagdown \\ \text{---} \end{array} = \begin{array}{c} \text{---} \cdot \\ \diagup \quad \diagdown \\ \text{---} \end{array} = \begin{array}{c} \text{---} \\ \diagup \quad \diagdown \\ \text{---} \cdot \end{array} \quad \text{and} \quad \begin{array}{c} \diagdown \\ \diagup \\ \diagdown \\ \diagup \end{array} = \begin{array}{c} \diagdown \\ \diagup \\ \diagdown \\ \diagup \cdot \end{array},$$

Moreover, arguably the most exciting relation is (2A.15), which, in spine pictures, is

$$\begin{array}{c} \text{---} \cdot \\ \text{---} \cdot \\ \text{---} \cdot \end{array} = \begin{array}{c} \text{---} \cdot \\ \text{---} \cdot \\ \text{---} \cdot \end{array} \quad \left(\text{closed version: } \begin{array}{c} \text{---} \\ \text{---} \\ \text{---} \end{array} = \begin{array}{c} \text{---} \\ \text{---} \\ \text{---} \end{array} \right).$$

This is a well-known, famous, and surprising relation among surfaces.

Remark 2A.17. As explained in [CT26b], we note that the boundaries of all cobordisms in \mathbf{MCob} are oriented with fixed orientation, which differs from the notion of unoriented cobordisms presented in e.g. [Cze24, Tub14, TT06]; in particular, we do not consider orientation-reversing diffeomorphisms of the boundaries. \diamond

The category \mathbf{MCob} is symmetric and pivotal, using the swap and the pivotal structure induced by cup/cap (use $\Delta \circ \eta$ and $\epsilon \circ \mu$) as the relevant structures. We will always use these as structures, or obvious analogs, whenever we work with \mathbf{MCob} or related categories.

Example 2A.18. Consider the following example:

$$\begin{array}{c} \uparrow \\ \text{---} \\ \text{---} \\ \text{---} \\ \uparrow \end{array} \quad \begin{array}{c} \uparrow \\ \text{---} \\ \text{---} \\ \text{---} \\ \text{---} \\ \text{---} \\ \text{---} \\ \uparrow \quad \uparrow \end{array} \quad \in \quad \text{Hom}_{\mathbf{MCob}}(2, 2),$$

where the orientation conventions for the boundary \mathbb{S}^1 are indicated by the arrows. As usual, we consider individual cobordisms as representatives for their corresponding diffeomorphism class. \diamond

2B. The linear algebra version. Let R be a commutative ring. Let $R\mathbf{Mod}$ be the symmetric monoidal category of finite-dimensional free R -modules (finite-dimensional vector spaces if R is a field) with the usual tensor product as the structure.

Definition 2B.1. A *Möbius topological quantum field theory*, or *MTQFT*, is a symmetric monoidal functor $\mathcal{F}: \mathbf{MCob} \rightarrow R\mathbf{Mod}$. \diamond

Remark 2B.2. We could be more general in Definition 2B.1 by using finitely-generated projective R -modules instead of finite-dimensional free R -modules. \diamond

Note that one can use the pivotality of \mathbf{MCob} to put a pairing on the R -modules in $\mathcal{F}(\mathbf{MCob})$.

Example 2B.3. Fix $R = \mathbb{Z}[\frac{1}{3}]$. Consider the MTQFT defined by $\mathcal{F}(1) = R[y]/(y^3)$ on objects. On morphisms, $\mathcal{F}(\mu)$ is the usual polynomial ring multiplication with unit $\mathcal{F}(\eta)(1) = 1$, and given a basis $\{1, y, y^2\}$ for $R[y]/(y^3)$, $\mathcal{F}(\epsilon)(y^2) = 3$ and zero on the other basis elements. Furthermore, we have

$$\begin{aligned} \mathcal{F}(\Delta)(1) &= \frac{1}{3}(1 \otimes y^2 + y \otimes y + y^2 \otimes 1), & \mathcal{F}(\Delta)(y) &= \frac{1}{3}(y \otimes y^2 + y^2 \otimes y), & \mathcal{F}(\Delta)(y^2) &= \frac{1}{3}y^2 \otimes y^2, \\ \mathcal{F}(m)(1) &= y, & \mathcal{F}(m)(y) &= y^2, & \mathcal{F}(m)(y^2) &= 0, \end{aligned}$$

and $\mathcal{F}(s)$ is the usual swap map for tensor products of modules. \diamond

Note the appearance of $\frac{1}{3}$, which looks a bit surprising at first glance. However, it is really an artifact of the relation (2A.15).

Remark 2B.4. Let us compare briefly with the standard Turaev–Turner framework for unoriented two-dimensional TQFTs [TT06]. In that setting, the algebraic input is an extended Frobenius algebra: besides the Frobenius structure, there is an orientation-reversing involution, often denoted

ϕ , together with a Möbius element. The resulting structure has been used and developed in several directions; see e.g. [CKQW25, GRY24].

Our convention is slightly different. The boundary circles in our cobordism category have fixed orientations, and we do not use the twist ϕ itself as a gluing operation. What remains visible in our diagrammatics is the Möbius generator. While we lose the boundary-orientation bookkeeping present in the full Turaev–Turner setting, which essentially amounts to a $\mathbb{Z}/2\mathbb{Z}$ factor, the advantage, in our opinion, is that the resulting diagrammatics are simpler: they form a plain diagram-algebra-style calculus, with the Möbius generator appearing as an ordinary local diagrammatic operation. \diamond

3. GRAPH INVARIANTS

We now define graph homologies. The following section is strongly inspired by [BM23], but also by [HGR05] and related works. We expect that the reader has basic background in graph theory, standard constructions in quantum topology, and link homologies. See e.g. [LZ04], [Tub25, TV17], and [Kho00, BN05] for some references.

3A. Preliminaries. We begin by recalling some relevant terminology.

Notation 3A.1. By *graph* we mean an undirected multigraph i.e. $G = (V, E, r)$ where V is a nonempty set of vertices, E a set of edges, and $r : E \rightarrow \{\{v_1, v_2\} : v_1, v_2 \in V\}$ (using multiset notation, we write $e = \{1, 2\}$ for $r(e) = \{1, 2\}$ etc.). Also, we require that $|V|, |E| < \infty$ i.e. finite graphs only. \diamond

Definition 3A.2. A *ribbon graph of a graph* G is an embedding $i : G \rightarrow \Gamma$, where Γ is a surface with boundary that deformation retracts onto $i(G)$. We refer to G as the *underlying graph* of Γ and to Γ as the *associated surface* of the ribbon graph. \diamond

We stress that such an embedding is extra structure: every graph can be made into a ribbon graph, potentially in multiple ways.

Example 3A.3. Here is an example:

$$G = (\{1, 2\}, \{\{1, 1\}, \{1, 2\}, \{1, 2\}\}), \quad \Gamma = \text{[Diagram: A surface with two vertices represented as thickened circles. The left vertex has a self-loop edge. The two vertices are connected by two parallel edges, one above and one below. The top edge is thickened to form a semi-circular arc connecting the two vertices.]}$$

where we have thickened up the (images of the) vertices for readability, as we will do throughout. \diamond

An orientation of a ribbon graph $i : G \rightarrow \Gamma$ is given by an orientation of its associated surface Γ , if it exists. Furthermore, let $\bar{\Gamma}$ denote the closed surface obtained by attaching discs to the boundary of Γ . Two ribbon graphs $i_1 : G_1 \rightarrow \Gamma_1$ and $i_2 : G_2 \rightarrow \Gamma_2$ are *equivalent* ribbon graphs if there is a homeomorphism $f : \bar{\Gamma}_1 \rightarrow \bar{\Gamma}_2$ that induces an isomorphism of graphs from G_1 to G_2 .

Notation 3A.4. It is customary to denote a ribbon graph $i : G \rightarrow \Gamma$ simply by the associated surface Γ . \diamond

In fact, one can represent oriented ribbon graphs as graphs in the plane, with vertices drawn as black dots and edges as curves, and at any one point, at most two of such curves can intersect. We call such a diagram a *ribbon diagram*. Every oriented ribbon graph has many associated ribbon diagrams. Moreover, we recall the following Reidemeister-type theorem for ribbon graphs:

Lemma 3A.5. *Two ribbon diagrams represent equivalent oriented ribbon graphs if and only if they are related by a finite sequence of **planar isotopy**, **Reidemeister(-type) moves** and **fork moves**. The planar isotopies are of the form (this is not an exhaustive list):*

$$(3A.6) \quad \text{[Diagram: Three pairs of moves. 1. A curve with a loop on the left is equivalent to a straight line. 2. A curve with a loop on the right is equivalent to a straight line. 3. A curve with a loop on the left is equivalent to a curve with a loop on the right.]}$$

The Reidemeister-type moves mirror the three Reidemeister moves for edges away from the vertices, i.e.

$$(3A.7) \quad \text{[Diagram: Three pairs of moves. 1. A loop on a vertical line is equivalent to the vertical line. 2. A crossing of two vertical lines is equivalent to the vertical lines. 3. A crossing of two vertical lines with a twist is equivalent to the vertical lines with a different twist.]}$$

while the fork move at vertices is given by

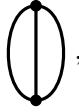
$$(3A.8) \quad \begin{array}{c} \cdots \\ \diagup \quad \diagdown \\ \cdot \\ \diagdown \quad \diagup \\ \cdots \end{array} \longleftrightarrow \begin{array}{c} \cdots \\ \diagdown \quad \diagup \\ \cdot \\ \diagup \quad \diagdown \\ \cdots \end{array}$$

We call all of these taken together as the **ribbon moves**.

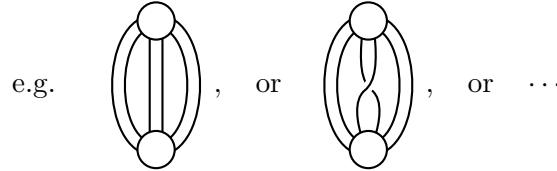
Proof. This is a nontrivial theorem, see e.g. [BKR22, Theorem 2.7]. The only difference for us is (3A.8); [BKR22] only considers ribbon graphs whose underlying graphs are trivalent, but the argument is identical in the more general setting (recall that a graph is **trivalent** or **cubic** if every vertex has degree three). \square

A ribbon diagram can be used to obtain a ribbon graph by using discs for vertices and bands for edges, as illustrated in Example 3A.9 below.

Example 3A.9. Given the ribbon diagram



we can associate a ribbon graph with underlying graph $G = (V, E, r)$, with vertices $V = \{0, 1\}$ and edges $E = \{e, f, g\}$ with $e = f = g = \{0, 1\}$, and associated surface



where half twists may be added to the bands resulting in a potentially nonorientable surface i.e. there may be many choices of associated surface for a given underlying graph. \diamond

Notation 3A.10. We will not use unoriented ribbon graphs in this paper, and we will say ribbon graph instead of oriented ribbon graph for short. \diamond

Remark 3A.11. In the case of unoriented ribbon graphs, we obtain an almost identical correspondence except that ribbon diagrams are replaced with signed ribbon diagrams. For our purposes though, we only consider oriented ribbon graphs, which we will think of as equivalence classes of ribbon diagrams related by ribbon moves and planar isotopy. \diamond

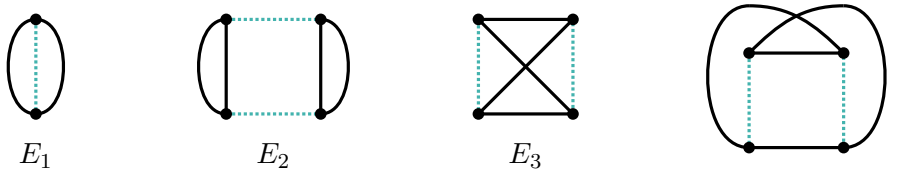
We now come to our main object of study. First, we recall the following:

Definition 3A.12. A **perfect matching** of a graph $G = (V, E, r)$ is a subset of edges $M \subset E$ such that each vertex is incident to exactly one edge in M . \diamond

Example 3A.13. Given the graph $G = (V, E, r)$ from Example 3A.9, the set $M = \{f\}$ gives a perfect matching of G ; $M = \{e\}$, or $M = \{g\}$ would also work. \diamond

Definition 3A.14. A **perfect matching graph**, denoted Γ_M , is a ribbon graph $i : G \rightarrow \Gamma$ together with a perfect matching M of the underlying graph G . The perfect matching is represented using blue dotted edges on the corresponding ribbon diagrams. \diamond

Example 3A.15. Examples of perfect matching graphs are given below:



where we note that the final two perfect matching graphs are equivalent; we leave it as an exercise to verify this. \diamond

Definition 3A.16. Two perfect matching graphs are **equivalent** if they are equivalent as ribbon graphs and the induced isomorphism of their underlying graphs preserves the perfect matching. \diamond

Notation 3A.17. From now on, we only consider ribbon graphs with connected underlying graphs $G = (V, E, r)$ with E nonempty; in particular, all vertices have degree at least one. \diamond

Given any ribbon graph, we can construct a canonical perfect matching graph, whose underlying graph is trivalent, by altering the vertices as follows:

Definition 3A.18. The *blowup* of a ribbon graph is obtained by replacing every vertex with vertices arranged in a circle:



where one uses as many vertices as the degree of the start vertex. \diamond

Lemma 3A.19. *The blowup of a ribbon graph is trivalent and admits a perfect matching. Moreover, if two ribbon graphs are equivalent, then so are their blowups.*

Proof. The first statement is immediate by construction, and there is a perfect matching that can be associated with the blowup by using the edges of the original graph, e.g.



For the second statement, let Γ_1, Γ_2 be two equivalent ribbon graphs, with Γ_1^b, Γ_2^b their respective blowups. Away from the vertices, Γ_2 is obtained from Γ_1 using a finite sequence of planar isotopy (3A.6) and Reidemeister moves (3A.7), and it is easy to see that the same is true of Γ_2^b and Γ_1^b . At the vertices, we simply note that e.g.



where we have used the final ribbon move (3A.8) three times to move the unattached edge across the three vertices on the blowup, and similarly for starting vertices of other degrees. \square

Thus, by Lemma 3A.19, we can and will restrict to ribbon graphs whose underlying graphs are trivalent with at least one perfect matching.

3B. Polynomial invariants. We now consider a generic polynomial invariant of ribbon graphs using specified relations.

Definition 3B.1. Let G be a trivalent graph with perfect matching M , and let Γ_M be a perfect matching graph with underlying graph G . The element $\langle \Gamma_M \rangle \in \mathbb{Z}[A, B, C]$, called the *bracket* (or *Penrose bracket polynomial*) of Γ_M , is characterized by:

$$(3B.2) \quad \left\langle \begin{array}{c} \diagup \quad \diagdown \\ \bullet \quad \bullet \\ \vdots \\ \bullet \quad \bullet \\ \diagdown \quad \diagup \end{array} \right\rangle = A \left\langle \begin{array}{c} | \quad | \\ | \quad | \end{array} \right\rangle + B \left\langle \begin{array}{c} X \\ X \end{array} \right\rangle,$$

$$(3B.3) \quad \left\langle \begin{array}{c} \bigcirc \end{array} \right\rangle = C,$$

$$(3B.4) \quad \langle \Gamma_1 \sqcup \Gamma_2 \rangle = \langle \Gamma_1 \rangle \cdot \langle \Gamma_2 \rangle.$$

Resolving a perfect matching edge by \parallel is called a *0-smoothing* and by χ a *1-smoothing*. \diamond

Definition 3B.1 is inspired by [Pen71], which is the case with $A = 1, B = -1$ in (3B.2) and $C = 3$ in (3B.3). By [Kho00], it is now mandatory to ask whether one can categorify (3B.2)–(3B.4), so we do this below.

Remark 3B.5. In order for the l.h.s. of (3B.3) to make sense as a bracket, we should also include the circle and disjoint unions of circles in the plane, up to a finite sequence of Reidemeister moves and planar isotopy, as additional equivalence classes in addition to the ribbon graphs. \diamond

Remark 3B.6. The bracket can of course be defined for any ribbon graph by using the canonical perfect matching induced from the blowup and Lemma 3A.19. \diamond

Proposition 3B.7. *The bracket is a ribbon graph invariant.*

Proof. Recall the relations in (3A.6), (3A.7) and (3A.8); the ribbon moves. We are required to show that if Γ_M and $\Gamma_{M'}$ are equivalent perfect matching graphs, i.e. there exists a finite sequence of ribbon moves that takes Γ_M to $\Gamma_{M'}$, then $\langle \Gamma_M \rangle = \langle \Gamma_{M'} \rangle$. Therefore, if we can show that the ribbon moves do not affect the evaluation of the skein relations (3B.2)–(3B.4), then we are done, since we can of course use them freely away from the evaluation sites.

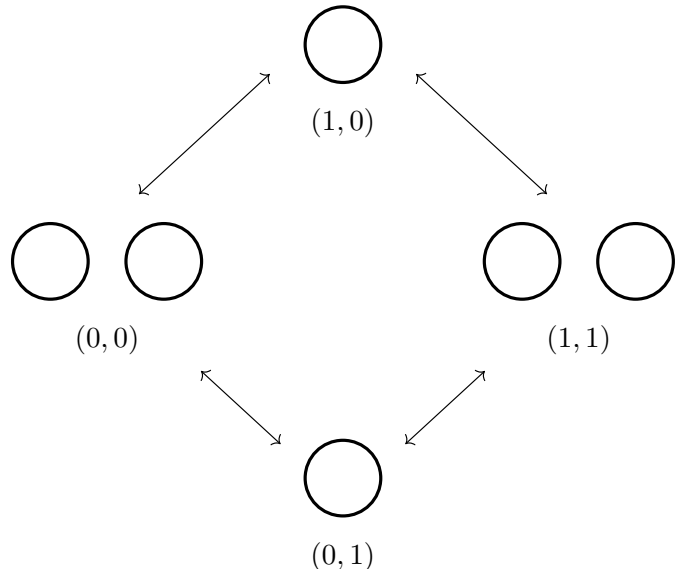
We first note that (3B.4) is true regardless of what form Γ_1 and Γ_2 take. Also, the evaluation of the circle in (3B.3) is not affected by Reidemeister moves or planar isotopy by construction as discussed in Remark 3B.5. Finally, it is clear that planar isotopies, and Reidemeister moves away from the perfect matching edge, do not affect the evaluation in (3B.2). The only part left to prove is then

where the marked red edge can either be a perfect matching or generic edge. On both sides, the 0-smoothing term in (3B.2) is clearly unchanged, while for the 1-smoothing term, equality follows directly from the third Reidemeister move. \square

Up to this point, we have not shown that the bracket is well-defined i.e. the order in which we resolve the perfect matching edges does not affect the result. In order to do so, we make use of the concept of a **hypercube of states**. The setup is as follows: let $G = (V, E, r)$ be a trivalent graph, $M = \{e_1, e_2, \dots, e_\ell\} \subset E$ be a perfect matching of G , and let Γ_M be a perfect matching graph with underlying graph G . By construction, note that $\ell = |V|/2$. If we resolve each perfect matching edge e_i by either a 0- or 1-smoothing, we obtain a set of circles in the plane called a **state** of Γ_M , and there are 2^ℓ of them. Given $\alpha = (\alpha_1, \alpha_2, \dots, \alpha_\ell) \in \{0, 1\}^\ell$, we let Γ_α denote the state of Γ_M where the perfect matching edge e_i has been resolved by an α_i -smoothing.

We can arrange the states Γ_α as vertices in a hypercube as shown in the following example.

Example 3B.8. Given the perfect matching graph E_2 from Example 3A.15, which has two perfect matching edges, we have $2^2 = 4$ states $\Gamma_{(0,0)}$, $\Gamma_{(1,0)}$, $\Gamma_{(0,1)}$, and $\Gamma_{(1,1)}$; these states have 2, 1, 1, and 2 circles respectively. It is useful to visualize the hypercube of states as follows:



This should come to no surprise for readers familiar with [Kau87, Kho00]. \diamond

In general, we can arrange states with constant $|\alpha| = \alpha_1 + \alpha_2 + \dots + \alpha_\ell$ as columns, with $|\alpha|$ increasing from left to right; note that the order in which states appear within a fixed column is arbitrary, and that $0 \leq |\alpha| \leq \ell$. Of course, the use of columns in this manner is simply a useful visualization tool, and in practice, the symmetry of the hypercube is undisturbed. The bidirectional arrows, which correspond to edges of the hypercube, appear between states Γ_α and $\Gamma_{\alpha'}$ if and only if α and α' differ on a single component.

Lemma 3B.9. *The hypercube of states is a ribbon graph invariant.*

Proof. From the proof that the skein relation (3B.2) is invariant under ribbon moves and planar isotopy in Proposition 3B.7, we know that 0- and 1-smoothings are invariant separately, and so the result follows. \square

Finally, to each vertex corresponding to some state Γ_α in the hypercube of states, we associate the quantity $A^{\ell-|\alpha|}B^{|\alpha|}C^{k_\alpha}$, where k_α is the number of circles in Γ_α , and then sum over all the vertices.

Lemma 3B.10. *The result $\sum_\alpha A^{\ell-|\alpha|}B^{|\alpha|}C^{k_\alpha}$ is $\langle \Gamma_M \rangle$. Since the order in which the vertices are summed has no effect, $\langle \Gamma_M \rangle$ is therefore well-defined.*

Proof. This is straightforward to see. \square

3C. Graph homology. We can obtain another ribbon graph invariant using homology, from which the bracket emerges for specific choices of A , B , and C , and which is strictly more powerful; the story is analogous to the emergence of the Jones polynomial from Khovanov homology in knot theory. We do so by enforcing certain conditions on our MTQFTs in order to build an invariant chain complex whose graded Euler characteristic is the bracket.

First suppose that we are given an MTQFT $\mathcal{F} : \mathbf{MCob} \rightarrow R\mathbf{Mod}$ with $\mathcal{F}(1) = V$. Let \mathcal{G} be a finitely-generated abelian group with generators g_1, g_2, \dots, g_m . Suppose that the finite-dimensional free R -module V has a \mathcal{G} -grading i.e. $V = \bigoplus_{g \in \mathcal{G}} V_g$ with \mathcal{G} considered as a set and only finitely many V_g are nonzero. Given a tuple $s = (s_1, s_2, \dots, s_m)$ of integers and an element $g = g_1^{p_1} g_2^{p_2} \dots g_m^{p_m} \in \mathcal{G}$ for some integers p_1, p_2, \dots, p_m , we can always shift the grading by setting $(V\{s\})_g = V_{g'}$ where $g' = g_1^{p_1-s_1} g_2^{p_2-s_2} \dots g_m^{p_m-s_m}$. The **graded dimension** of V is then a polynomial in the variables q_1, q_2, \dots, q_m given by

$$q\dim(V) = \sum_{g \in \mathcal{G}} q_1^{p_1} q_2^{p_2} \dots q_m^{p_m} \dim(V_g).$$

Example 3C.1. For $\mathcal{G} = \mathbb{Z}/n\mathbb{Z} \times \mathbb{Z}/2\mathbb{Z}$ this really means we have two grading variables, say q and b , that satisfy $q^n = 1 = b^2$. In this case the grading would be a tuple (x, y) where we read the first entry modulo n and the second modulo 2. We will use similar conventions for other gradings. \diamond

Further suppose that the following relation holds on V :

$$(3C.2) \quad \mathcal{F}(m^2) = \mathcal{F}(h),$$

which is a more restricted relation than (2A.15) on \mathbf{MCob} ; in particular, \mathcal{F} is not faithful.

Remark 3C.3. The relation (3C.2) may look a bit mysterious at first. Topologically, the relation is $m^3 = hm$, cf. (2A.15), and replacing this by $m^2 = h$ would amount to the identity

$$\left(\text{Klein bottle with two red arrows} \right) = \left(\text{torus} \right) \quad (\text{not a topological identity}).$$

In other words, it would identify the Klein bottle with the torus, which is, of course, not true.

The reason that (3C.2) can nevertheless hold in our examples is that we are no longer working faithfully with the topological monoid. Roughly speaking, and with Green relations/cells [Gre51] in mind (using the convention of [KST24]), we pass to a higher cell of the monoid $\langle m, h \mid m^3 = hm, mh = hm \rangle$, where m becomes locally invertible. In that setting one may cancel the remaining m , giving the effective relation $m^2 = h$. Alternatively, the respective monoid algebra is sandwich cellular in the sense of [Tub24b], so one can use the standard cell theory to “cut out” the relevant parts. We call this **pseudo-invertibility**.

Concrete solutions are given in Section 5. \diamond

We are now ready to begin constructing our chain complex. Fix a perfect matching graph Γ_M with trivalent underlying graph $G = (V, E, r)$ and perfect matching $M = \{e_1, e_2, \dots, e_\ell\} \subset E$. Form the hypercube of states as shown e.g. in Example 3B.8. We now give the edges a fixed direction according to the following rule: there is a directed edge $\Gamma_\alpha \rightarrow \Gamma_{\alpha'}$ if and only if $|\alpha'| = |\alpha| + 1$. To each state Γ_α , we then associate the \mathcal{G} -graded R -module $V_\alpha = \otimes^{k_\alpha} V\{s|\alpha\}$ where k_α is the number of circles in Γ_α and s is some constant shift. Define a complex $C^{*,*}(\Gamma_M)$ by

$$(3C.4) \quad C^{i,*}(\Gamma_M) = \bigoplus_{\alpha \in \{0,1\}^\ell, |\alpha|=i} V_\alpha,$$

and it is trivial outside of $i = 1, \dots, \ell$. $C^{i,*}(\Gamma_M)$ is also \mathcal{G} -graded with $C^{i,g}(\Gamma_M) = (C^{i,*}(\Gamma_M))_g$.

Remark 3C.5. Given a shift $s = (s_1, s_2, \dots, s_m)$, we define $s|\alpha| = (s_1|\alpha|, s_2|\alpha|, \dots, s_m|\alpha|)$ i.e. component-by-component multiplication. \diamond

Remark 3C.6. We will also think of the complex $C^{*,*}(\Gamma_M)$ as arranged in a hypercube, with vertices and directed edges in bijective correspondence with those in the hypercube of states, i.e. $\Gamma_\alpha \leftrightarrow V_\alpha$ for vertices and $\Gamma_\alpha \rightarrow \Gamma_{\alpha'} \leftrightarrow V_\alpha \rightarrow V_{\alpha'}$ for directed edges. \diamond

Example 3C.7. Given the hypercube of states from [Example 3B.8](#), the corresponding complex can also be visualized as follows:

$$\begin{array}{ccccc}
 & & V\{s\} & & \\
 & \nearrow^{\mu_V} & & \searrow_{\Delta_V} & \\
 V \otimes V & & \oplus & & V \otimes V\{2s\} \\
 & \searrow_{\mu_V} & & \nearrow_{\Delta_V} & \\
 & & V\{s\} & & \\
 i = 0 & & i = 1 & & i = 2
 \end{array}$$

where the interpretation of directed edges as R -linear maps is discussed below. \diamond

Remark 3C.8. In forming our complex, the symmetry of the hypercube of states is destroyed; there is a preferred direction that runs from the vertex with $|\alpha| = 0$ to the vertex with $|\alpha| = \ell$. Rotating about the preferred axis gives a residual symmetry for states with fixed $|\alpha|$, which is preserved in the complex up to reordering of the direct sum. \diamond

We now define the differential

$$\partial^i: C^{i,*}(\Gamma_M) \longrightarrow C^{i+1,*}(\Gamma_M).$$

Fix a directed edge in the cube of states, say from Γ_α to $\Gamma_{\alpha'}$, where α' is obtained from α by changing one 0-smoothing into a 1-smoothing. Away from this smoothing, the two states are identical. At the smoothing itself, exactly one of the following three things happens:

$$\begin{array}{ccc}
 \text{merge} & \text{split} & \text{funny edge} \\
 \bigcirc \quad \bigcirc \xrightarrow{\mu_V} \bigcirc & \bigcirc \xrightarrow{\Delta_V} \bigcirc \quad \bigcirc & \bigcirc \xrightarrow{m_V} \infty
 \end{array}$$

Here the pictures only show the components affected by the chosen edge of the cube; all other components are unchanged and contribute identity tensor factors. The first two cases are the familiar ones from ordinary link homology: two circles merge, or one circle splits into two. The third case is the new feature in the present setting: one circle remains one circle, but acquires a self-crossing; this edge is represented algebraically by the Möbius map.

Remark 3C.9. The reader familiar with virtual link homology might recognize the funny edge, which always causes trouble, see [\[Man07\]](#) for an early reference for this. \diamond

Using the correspondence from [Remark 3C.6](#), we therefore assign to the directed edge $\Gamma_\alpha \rightarrow \Gamma_{\alpha'}$ the R -linear map

$$\partial_{\alpha\alpha'}: V_\alpha \longrightarrow V_{\alpha'}$$

given by

$$\partial_{\alpha\alpha'} = \begin{cases} \mu_V \otimes id, & \text{if two circles merge,} \\ \Delta_V \otimes id, & \text{if one circle splits into two,} \\ m_V \otimes id, & \text{if one circle crosses itself,} \end{cases}$$

where $\mu_V = \mathcal{F}(\mu)$, $\Delta_V = \mathcal{F}(\Delta)$, and $m_V = \mathcal{F}(m)$, and where the identity factors act on the unchanged circle components.

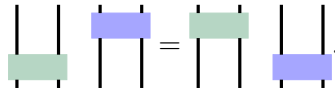
Remark 3C.10. There may be some concern over the ordering of the tensor product of R -linear maps along directed edges of the complex. We note that any such choice ultimately corresponds to an ordering of the circles in the hypercube of states; the result is identical up to an overall application of a tensor product swap map. \diamond

We have the following crucial proposition:

Proposition 3C.11. *For any perfect matching graph Γ_M , the complex $C^{*,*}(\Gamma_M)$ together with the maps $\partial_{\alpha\alpha'}$ form a commutative diagram.*

Proof. We first note that if the square faces of our complex commute, then clearly the whole complex commutes by construction. For each face, consider opposing vertices such that the directed edges move away from one vertex in two directions and towards the other vertex from two directions e.g. $V \otimes V$ and $V \otimes V\{2s\}$ form opposing vertices in [Example 3C.7](#).

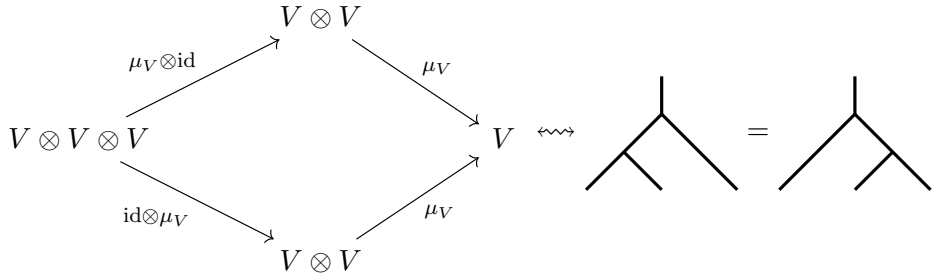
Given a face, we begin by noting that if one path between opposing vertices contains a composition of maps with the μ_V , Δ_V , or m_V operating on different copies of V in the tensor product, it is relatively straightforward to see that the other path must contain the same composition of maps with the order swapped; using spine diagrams, this is essentially



By the functorial properties of the tensor product, the face must therefore commute.

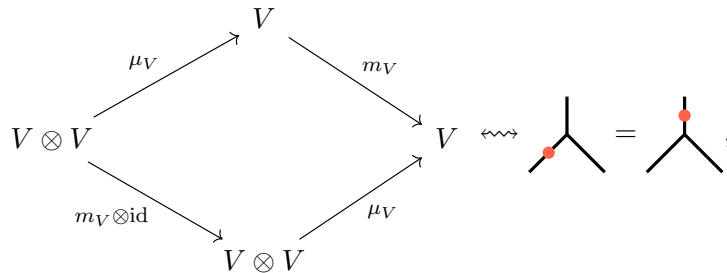
It remains to consider the case where both paths between two opposing vertices in a square face involve maps acting on the same circle components. We suppress all unaffected components, which only contribute identity tensor factors, and everything that is not relevant for the discussion. By construction, the tensor powers at the two opposing vertices can differ by 0, 1, or 2.

If the tensor powers differ by 2, then both paths are built only from merges, or dually only from splits. A typical merge–merge face is



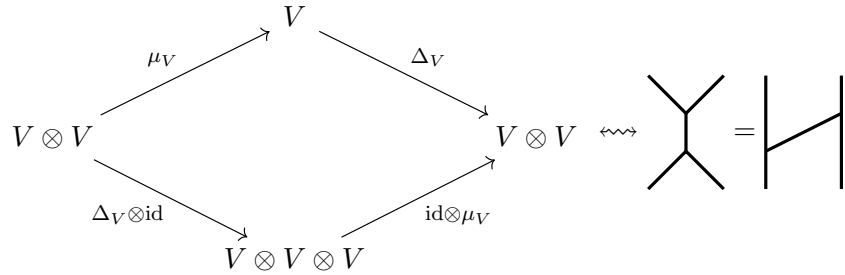
which commutes by associativity. The dual split–split face commutes by coassociativity.

If the tensor powers differ by 1, then one of the two local changes is a merge or split, while the other is a Möbius change. For instance, a typical merge–Möbius face is

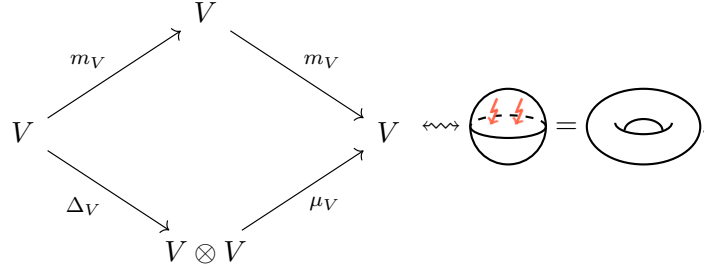


and this commutes by the indicated relation. The other faces of this type commute by the analogous relations.

Finally, suppose that the tensor powers at the opposing vertices are equal. These are always the most exciting faces. A prototypical face without m_V is

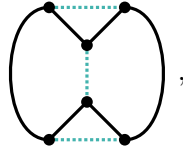


which commutes by the displayed Frobenius $H=I$ relation. The only nontrivial new face is

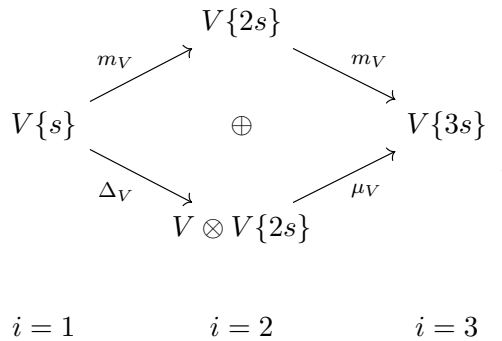


The two paths around this face are m_V^2 and $\mu_V \circ \Delta_V$, so this face commutes exactly by pseudo-invertibility (3C.2), as displayed. \square

Example 3C.12. The following example shows that we actually do require the pseudo-invertibility condition (3C.2) in Proposition 3C.11. Consider the perfect matching graph:



which indeed contains the following face in its corresponding complex:



as one can easily check. \diamond

Let us now define the differential ∂^i . For $v \in V_\alpha \subset C^{i,*}(\Gamma_M)$, we define

$$(3C.13) \quad \partial^i(v) = \sum_{\alpha'} (-1)^{f_{\alpha\alpha'}} \partial_{\alpha\alpha'}(v),$$

where the sum is over all α' such that there is a directed edge $\Gamma_\alpha \rightarrow \Gamma_{\alpha'}$ and $f_{\alpha\alpha'}$ counts the number of 1s to the left of the component where α and α' differ. Clearly, $\partial^i(v) \in C^{i+1,*}(\Gamma_M)$.

Theorem 3C.14. $(C^{i,*}(\Gamma_M), \partial^i)$ is a chain complex.

Proof. We already know that $\partial^i : C^{i,*}(\Gamma_M) \rightarrow C^{i+1,*}(\Gamma_M)$ is a R -linear map between R -modules, and so we only need to show that $\partial^{i+1} \circ \partial^i = 0$. But we know from Proposition 3C.11 that the faces of the complex commute, and so the signs $(-1)^{f_{\alpha\alpha'}}$ chosen in (3C.13) are such that the faces now anticommute. The result then follows. \square

Furthermore, if we also require that the maps μ_V , Δ_V , and m_V preserve the \mathcal{G} -grading up to a constant shift s , then ∂ also does the same, which is then compensated by the shift s in \mathcal{G} -grading when moving between R -modules V_α and $V_{\alpha'}$ with $|\alpha'| = |\alpha| + 1$ in the complex; in other words, ∂ has bigrading $(1, 0)$.

We can now define the homology of our complex as follows.

Definition 3C.15. Let G be a trivalent graph with perfect matching M , and let Γ_M be a perfect matching graph with underlying graph G . The *Möbius homology* of Γ_M is

$$MH^{i,g}(\Gamma_M; R) = \frac{\ker \partial : C^{i,g}(\Gamma_M) \rightarrow C^{i+1,g}(\Gamma_M)}{\operatorname{im} \partial : C^{i-1,g}(\Gamma_M) \rightarrow C^{i,g}(\Gamma_M)},$$

which is a \mathcal{G} -graded R -module. \diamond

The additional (homological) grading variable is denoted by t .

Remark 3C.16. As in the case of the bracket (also see [Remark 3B.6](#)), we can define the Möbius homology for any ribbon graph by using the canonical perfect matching induced from the blowup and [Lemma 3A.19](#). \diamond

Finally, we have the following theorem:

Theorem 3C.17. *The graded (Hilbert-)Poincaré polynomial*

$$(3C.18) \quad Mh(\Gamma_M) = \sum_i t^i q \dim(MH^{i,*}(\Gamma_M; R))$$

associated with the Möbius homology is a ribbon graph invariant. Furthermore, the graded Euler characteristic of the underlying chain complex is the bracket with $A = 1$, $B = -q_1^{s_1} q_2^{s_2} \cdots q_m^{s_m}$, and $C = q \dim(V)$.

Proof. Firstly, we know that the hypercube of states is a ribbon graph invariant. Furthermore, the preferred direction from the all 0-smoothing state $|\alpha| = 0$ to the all 1-smoothing state $|\alpha| = \ell$ is independent of the choice of labeling for the perfect matching edges. By [Remark 3C.8](#), the residual symmetry, when translated to the complex $C^{*,*}(\Gamma_M)$, amounts to a reordering of the direct sum of R -modules V_α with fixed $|\alpha|$. Furthermore, by [Remark 3C.10](#), we also know that the chain groups and maps are defined up to an overall application of a tensor product swap map. Lastly, any relabeling of the perfect matching edges may also affect the definition of ∂^i in [\(3C.13\)](#) by a relative minus sign. In any case, when taking the graded dimensions of the homology groups, the result is independent of any such choices.

To prove the second part of the statement, first note that $q \dim(V\{s\}) = q_1^{s_1} q_2^{s_2} \cdots q_m^{s_m} q \dim(V)$. Since all our R -modules are free of finite rank and ∂ preserves the \mathcal{G} -grading, the graded Euler characteristic of the chain complex $(C^{i,*}(\Gamma_M), \partial^i)$ is either given by the alternating sum of the graded dimensions of the $MH^{i,*}(\Gamma_M; R)$ or of the $C^{i,*}(\Gamma_M)$ themselves. Using the latter, we obtain a sum of terms $(-q_1^{s_1} q_2^{s_2} \cdots q_m^{s_m})^{|\alpha|} (q \dim(V))^{k_\alpha}$, which is exactly the bracket with the given choice of variables. \square

Later in [Section 6](#), we will see examples demonstrating that the Möbius homology, through the associated graded Poincaré polynomial, is strictly more powerful than the bracket as a ribbon graph invariant.

Remark 3C.19. It would be interesting to study the Möbius homology using an asymptotic or big data approach, as, for example, in [\[COT24, DGS25, KLTVZ25, TZ25\]](#). In particular, it would be interesting to have a weighting on the statement that the Möbius homology is strictly more powerful than the bracket. \diamond

Remark 3C.20. One of the strongest features of link homologies is that they are not only invariants of links, but also behave functorially under link cobordisms; see, for example, [\[BN05, CMW09, Jac04\]](#) or, quite generally, [\[ETW18\]](#). It is natural to ask for an analogous statement here: one would like suitable cobordisms between perfect matching ribbon graphs to induce maps on the homologies constructed in this paper. We do not pursue this in the present work, but the nonorientable cobordism model suggests that such a functorial extension should exist. \diamond

3D. Geometric complex. We briefly mention another way to obtain a ribbon graph invariant using the hypercube of states and nonorientable cobordisms, which is more geometric in nature. The result is similarly a chain complex with an associated homology, but we are able to relax the somewhat artificial condition (3C.2); the trade-off is that the chain groups have a somewhat more complicated structure with less flexibility.

We begin by considering the \mathbb{K} -linearization of \mathbf{MCob} , for some fixed field \mathbb{K} , with closed surfaces evaluated according to

$$(3D.1) \quad \begin{array}{c} \text{---} \\ \circ \\ \text{---} \end{array} = \alpha_0, \quad \begin{array}{c} \text{---} \\ \cup \\ \text{---} \end{array} = \alpha_1, \quad \begin{array}{c} \text{---} \\ \cup \cup \\ \text{---} \end{array} = \alpha_2, \quad \dots,$$

$$(3D.2) \quad \begin{array}{c} \text{---} \\ \cup \\ \text{---} \\ \downarrow \end{array} = \beta_0, \quad \begin{array}{c} \text{---} \\ \cup \\ \text{---} \\ \downarrow \end{array} = \beta_1, \quad \begin{array}{c} \text{---} \\ \cup \cup \\ \text{---} \\ \downarrow \end{array} = \beta_2, \quad \dots,$$

$$(3D.3) \quad \begin{array}{c} \text{---} \\ \cup \\ \text{---} \\ \downarrow \downarrow \end{array} = \gamma_0, \quad \begin{array}{c} \text{---} \\ \cup \\ \text{---} \\ \downarrow \downarrow \end{array} = \gamma_1, \quad \begin{array}{c} \text{---} \\ \cup \cup \\ \text{---} \\ \downarrow \downarrow \end{array} = \gamma_2, \quad \dots,$$

and the empty cobordism \emptyset is evaluated to $1 \in \mathbb{K}$. The coefficients in (3D.1)–(3D.3) are obtained from the following generating functions:

$$Z_\alpha = \frac{p_\alpha(T)}{q(T)} = \sum_{k \geq 0} \alpha_k T^k, \quad Z_\beta = \frac{p_\beta(T)}{q(T)} = \sum_{k \geq 0} \beta_k T^k, \quad Z_\gamma = \frac{p_\gamma(T)}{q(T)} = \sum_{k \geq 0} \gamma_k T^k,$$

where $q(T) = 1 - a_1 T + a_2 T^2 + \dots + (-1)^M a_M T^M \in \mathbb{K}(T)$ and furthermore, $p_\alpha(T), p_\beta(T), p_\gamma(T) \in \mathbb{K}[T]$ satisfy

$$(3D.4) \quad \deg(p_\beta(T)), \deg(p_\gamma(T)) < K = \max(\deg(p_\alpha(T)) + 1, M).$$

Next, we make use of the *universal construction* of [BHMV95] with the given closed surface evaluations (the surfaces listed are the only closed surfaces by (2A.15)) to construct the category $\mathbf{MCob}_{\alpha, \beta, \gamma}$, introduced in [CT26b]. From [CT26b, Proposition 3.11], we know that $\mathbf{MCob}_{\alpha, \beta, \gamma}$ is symmetric and pivotal, and has a generator-relation presentation with generators (2A.1) and (2A.2), and relations (2A.3)–(2A.12) and (2A.13)–(2A.15), together with the *handle relation*

$$\sigma = h^K + \sum_{i=1}^M (-1)^i a_i h^{K-i} = 0 \rightsquigarrow K \begin{array}{c} | \\ \bullet \\ | \end{array} - a_1 \cdot (K-1) \begin{array}{c} | \\ \bullet \\ | \end{array} \pm \dots + (-1)^{\deg q} a_{\deg q} \cdot (K - \deg q) \begin{array}{c} | \\ \bullet \\ | \end{array} = 0.$$

(The number next to the dot denotes its multiplicity.) In particular, the hom spaces of $\mathbf{MCob}_{\alpha, \beta, \gamma}$ are finite dimensional vector spaces whose elements contain a maximum of $K - 1$ handles. For more details on the construction of $\mathbf{MCob}_{\alpha, \beta, \gamma}$, see [CT26b].

Remark 3D.5. Here and in Section 3E, we use a field instead of a commutative ring only because [CT26b] did. This requirement can be relaxed if needed. \diamond

Let us now take $n \in \mathbb{N}_{>0}$. Suppose that we choose $p_\alpha(T)$ such that

$$\deg(p_\alpha(T)) = \begin{cases} n & n \text{ even,} \\ n-1 & n \text{ odd,} \end{cases}$$

and that $q(T) = 1 - T$. The handle relation then reads $h^{n+1} = h^n$ for n even, and $h^n = h^{n-1}$ for n odd i.e. $K = n + 1, n$ for n even, odd, respectively. We then choose $p_\beta(T), p_\gamma(T)$ such that (3D.4) is satisfied. We then have a family of categories $\mathbf{MCob}_{\alpha, \beta, \gamma}^n$ for each n .

We now build a chain complex for each n . Given a perfect matching graph Γ_M with trivalent underlying graph $G = (V, E, r)$ together with perfect matching $M = \{e_1, e_2, \dots, e_\ell\} \subset E$, we again consider the hypercube of states with directed edges as before. To each state with k_α circles, we associate the finite-dimensional vector space $V_{\alpha, n} = \text{hom}_{\mathbf{MCob}_{\alpha, \beta, \gamma}^n}(0, k_\alpha)$. We then define a complex $C_n^{*,*}(\Gamma_M)$ as in (3C.4) (we will come to the grading later); note that Remark 3C.6 and Remark 3C.8 also apply in this setting.

The differential $\partial_n^i : C_n^{i,*}(\Gamma_M) \rightarrow C_n^{i+1,*}(\Gamma_M)$ can also be constructed in the same manner as before: recall that there were three scenarios describing the change of state moving from one vertex

to another: *i*) two circles merge, *ii*) one circle splits in two, or *iii*) one circle crosses itself. We need to define linear maps representing these three scenarios. To begin, let

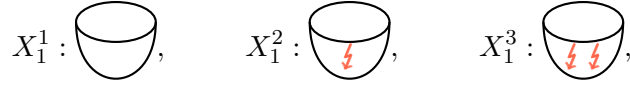
$$\zeta_n = \begin{cases} h^{n/2} \circ m & n \text{ even,} \\ h^{(n-1)/2} \circ m & n \text{ odd,} \end{cases}$$

be cobordisms i.e. $\zeta_n \in \text{End}_{\mathbf{MCob}_{\alpha,\beta,\gamma}^n}(1)$ for each n . Given elements $X_n \in \text{hom}_{\mathbf{MCob}_{\alpha,\beta,\gamma}^n}(0, 1)$ and $Y_n \in \text{hom}_{\mathbf{MCob}_{\alpha,\beta,\gamma}^n}(0, 2)$, we define the following linear maps:

$$\begin{aligned} \mu_n &: \text{hom}_{\mathbf{MCob}_{\alpha,\beta,\gamma}^n}(0, 2) \rightarrow \text{hom}_{\mathbf{MCob}_{\alpha,\beta,\gamma}^n}(0, 1), & Y_n &\mapsto \zeta_n \circ \mu \circ Y_n, \\ \Delta_n &: \text{hom}_{\mathbf{MCob}_{\alpha,\beta,\gamma}^n}(0, 1) \rightarrow \text{hom}_{\mathbf{MCob}_{\alpha,\beta,\gamma}^n}(0, 2), & X_n &\mapsto \Delta \circ \zeta_n \circ X_n, \\ m_n &: \text{hom}_{\mathbf{MCob}_{\alpha,\beta,\gamma}^n}(0, 1) \rightarrow \text{hom}_{\mathbf{MCob}_{\alpha,\beta,\gamma}^n}(0, 1), & X_n &\mapsto \zeta_n \circ X_n, \end{aligned}$$

and associate them with the directed edges corresponding to scenarios *i*), *ii*), and *iii*) respectively, tensored by the appropriate number of identity maps ([Remark 3C.10](#) also applies here).

Example 3D.6. For $n = 1$, $h_1 = 1_1$ i.e. there are no handles, and we have three basis vectors for $\text{hom}_{\mathbf{MCob}_{\alpha,\beta,\gamma}^1}(0, 1)$:



and we have

$$m_1: X_1^1: \text{circle} \mapsto \text{cylinder with lightning bolt} = X_1^2: \text{circle with lightning bolt},$$

and similarly for the other basis vectors and maps. \diamond

Recall from [Proposition 3C.11](#) that if we could get all the faces of our complex to commute, then the complex itself forms a commutative diagram; we would like to do the same here. Also recall from the corresponding proof that opposing vertices can have tensor powers differing by either *i*) 0, *ii*) 1, or *iii*) 2. Instead of tensor powers, in the present case we have the positive integer k_α appearing in $\text{hom}_{\mathbf{MCob}_{\alpha,\beta,\gamma}^n}(0, k_\alpha)$, which gives the number of circles in the corresponding state Γ_α in the hypercube of states.

Using identical reasoning as in the proof of [Proposition 3C.11](#), we only need to consider faces whose paths contain a composition of maps with μ_n , Δ_n , or m_n operating on the same circles. Faces corresponding to scenario *iii*) again must either trivially commute, or commute by associativity or coassociativity. Also, since handles and Möbius strip insertions move freely around cobordisms, faces corresponding to scenario *ii*) also commute. For scenario *i*), we again have that the only new nontrivial relation that must be satisfied is $m_n^2 = \mu_n \circ \Delta_n$, which holds automatically: both sides contain two Möbius strip insertions, and the r.h.s. contains an extra handle with respect to the l.h.s. that is then eliminated by the handle relation. By the classification of surfaces, we therefore conclude that they represent the same cobordism.

If we then define a differential ∂_n^i the same as in [\(3C.13\)](#), we can construct a chain complex by the same reasoning as in the proof of [Theorem 3C.14](#). Let us now define a grading by setting $\mathcal{G} = \mathbb{Z}/2\mathbb{Z}$. Given a positive integer k , the grading of an element $Z_n \in \text{hom}_{\mathbf{MCob}_{\alpha,\beta,\gamma}^n}(0, k)$ is given by 0(1) for an even(odd) number of Möbius strip insertions in total; note that the parity of Möbius strip insertions is respected by [\(2A.15\)](#), and so the grading is well-defined.

Example 3D.7. For $n = 1$ following [Example 3D.6](#), we have $\text{hom}_{\mathbf{MCob}_{\alpha,\beta,\gamma}^1}(0, 1) = W_0 \oplus W_1$ with $X_1^1, X_1^3 \in W_0$ and $X_1^2 \in W_1$. \diamond

The point is that the maps μ_n , Δ_n , and m_n all contain a single Möbius strip insertion; hence, the differential ∂_n^i preserves the $\mathbb{Z}/2\mathbb{Z}$ -grading up to a shift of size 1. By shifting the $\mathbb{Z}/2\mathbb{Z}$ -grading of each of the vector spaces $V_{\alpha,n}$ by the appropriate amount for each fixed $|\alpha|$, we then have that ∂_n has bigrading $(1, 0)$. Finally, we can define the homology as in [Definition 3C.15](#) and associated graded

Poincaré polynomial, which is a ribbon graph invariant for the same reasons given in the proof of the first part of [Theorem 3C.17](#). A more thorough analysis of the resulting invariant is left for future work.

3E. An integer graded version. The fact that the handle relation $h^{n+1} = h^n$ for n even, and $h^n = h^{n-1}$ for n odd, is monoid-like prevents us from obtaining a more interesting grading than $\mathcal{G} = \mathbb{Z}/2\mathbb{Z}$. As an alternative, let us return to working with \mathbf{MCob} instead of $\mathbf{MCob}_{\alpha,\beta,\gamma}$. In place of $\text{hom}_{\mathbf{MCob}_{\alpha,\beta,\gamma}^n}(0, k_\alpha)$, define the vector space V'_α as \mathbb{K} -linear combinations of cobordisms in $\text{hom}_{\mathbf{MCob}}(0, k_\alpha)$ whose connected components are all nonorientable. In place of μ_n, Δ_n , and m_n , define the maps

$$\begin{aligned} \mu &: \text{hom}_{\mathbf{MCob}}(0, 2) \rightarrow \text{hom}_{\mathbf{MCob}}(0, 1), & Y &\mapsto \mu \circ Y, \\ \Delta &: \text{hom}_{\mathbf{MCob}}(0, 1) \rightarrow \text{hom}_{\mathbf{MCob}}(0, 2), & X &\mapsto \Delta \circ X, \\ m &: \text{hom}_{\mathbf{MCob}}(0, 1) \rightarrow \text{hom}_{\mathbf{MCob}}(0, 1), & X &\mapsto m \circ X, \end{aligned}$$

extended \mathbb{K} -linearly. Given any element $X \in \text{hom}_{\mathbf{MCob}}(0, 1)$ whose connected components are all nonorientable, we must have an element $X' \in \text{hom}_{\mathbf{MCob}}(0, 1)$ with $X = m \circ X'$. Now notice that we have

$$(\mu \circ \Delta)(X) = \mu \circ \Delta \circ X = \mu \circ \Delta \circ m \circ X' = m^3 \circ X' = m^2 \circ X = m^2(X),$$

where we have used the relation [\(2A.15\)](#) in the third equality. Therefore, the problematic face commutes (the other face types commute trivially or using the relations in \mathbf{MCob} as previously) and we can again build a chain complex as before.

Furthermore, for the grading, set $\mathcal{G} = \mathbb{Z}$, and for each of the \circ - \otimes -generators of \mathbf{MCob} , assign the following integers $1_1, s : 0$, $\eta, \epsilon : -1$, and $\mu, \Delta, m : 1$. Define the grading of a cobordism in V'_α by decomposing it into a \circ - \otimes -product of generators, and summing over all the integers assigned to each generator appearing in the decomposition. Since the \mathbf{MCob} relations respect the given assignments (the reader is encouraged to check this), the grading is well-defined. Clearly, the differentials built from μ, Δ, m preserve the grading up to a shift of size 1.

Finally, we note that the V'_α are infinite dimensional as the genus of cobordisms may be unbounded. To produce a finite-dimensional space, we can form a subspace of each V'_α by restricting to cobordisms with a certain fixed genus or less. In addition, to ensure that the images of the maps comprising the differential lie in the relevant codomains, we must increase the maximum genus every second step in the chain to account for appearances of $h = \mu \circ \Delta$. We are then left with a choice of maximum genus $n \in \mathbb{N}$ for the first nonzero chain group.

Altogether, after taking the homology and forming the associated graded Poincaré polynomial, we have another family of ribbon graph invariants, one for each $n \in \mathbb{N}$, though this invariant appears to be much more difficult to compute in practice.

4. MÖBIUS FROBENIUS ALGEBRAS

We assume some familiarity with [\[Koc04\]](#) or similar references.

4A. Definition. In analogy with the ordinary Frobenius algebra and TQFT correspondence, we now establish a bijective correspondence that allows us to work with more compact objects, namely Frobenius algebras with some extra structure, instead of MTQFTs. We begin with the following definition.

Definition 4A.1. Let \mathcal{C} be a braided monoidal category. A *Möbius Frobenius algebra* in \mathcal{C} is a 6-tuple $(A, \mu_A, \eta_A, \Delta_A, \epsilon_A, m_A)$, where $(A, \mu_A, \eta_A, \Delta_A, \epsilon_A)$ is a commutative Frobenius algebra in \mathcal{C} and $m_A : A \rightarrow A$ is a morphism such that the diagrams

$$(4A.2) \quad \begin{array}{ccccc} A \otimes A & \xleftarrow{m_A \otimes \text{id}_A} & A \otimes A & \xrightarrow{\text{id}_A \otimes m_A} & A \otimes A \\ \mu_A \downarrow & & \downarrow \mu_A & & \downarrow \mu_A \\ A & \xleftarrow{m_A} & A & \xrightarrow{m_A} & A \end{array}$$

and

$$(4A.3) \quad \begin{array}{ccc} A & \xrightarrow{\Delta_A} & A \otimes A \\ m_A \uparrow & & \downarrow \mu_A \\ A & \xrightarrow{m_A^3} & A \end{array}$$

commute.

Two Möbius Frobenius algebras $(A, \mu_A, \eta_A, \Delta_A, \epsilon_A, m_A)$ and $(A', \mu_{A'}, \eta_{A'}, \Delta_{A'}, \epsilon_{A'}, m_{A'})$ are said to be *isomorphic* if there exists an isomorphism of commutative Frobenius algebras $f : A \rightarrow A'$ such that $m_{A'} \circ f = f \circ m_A$. \diamond

Remark 4A.4. The morphism $m_A : A \rightarrow A$ is not required to be a morphism of Frobenius algebras in the sense of [Koc04]; in particular, it need not preserve the unit or counit. \diamond

Example 4A.5. Take $n \in \mathbb{N}_{>0}$. Consider the subcategory of $\mathbb{K}\mathbf{Vec} = \mathbb{K}\mathbf{Mod}$ whose objects are given by $\text{hom}_{\mathbf{MCob}_{\alpha,\beta,\gamma}^n}(0, k)$ with k a positive integer (see Section 3D). The morphisms in $\text{hom}_{\mathbf{MCob}_{\alpha,\beta,\gamma}^n}(0, k) \rightarrow \text{hom}_{\mathbf{MCob}_{\alpha,\beta,\gamma}^n}(0, k')$ are given by $\text{hom}_{\mathbf{MCob}_{\alpha,\beta,\gamma}^n}(k, k')$ using composition in the same manner e.g. Example 3D.6; call the resulting category \mathcal{C} .

Now define a monoidal product in \mathcal{C} given on objects as

$$\text{hom}_{\mathbf{MCob}_{\alpha,\beta,\gamma}^n}(0, k) \square \text{hom}_{\mathbf{MCob}_{\alpha,\beta,\gamma}^n}(0, k') = \text{hom}_{\mathbf{MCob}_{\alpha,\beta,\gamma}^n}(0, k + k')$$

with unit object $\text{hom}_{\mathbf{MCob}_{\alpha,\beta,\gamma}^n}(0, 0) \cong \mathbb{K}$ and braiding given by appropriate insertions of s from (2A.1). On morphisms, \square is disjoint union of cobordisms. Given $V = \text{hom}_{\mathbf{MCob}_{\alpha,\beta,\gamma}^n}(0, 1)$, we have that \mathcal{C} is generated by the Möbius Frobenius algebra $(V, \mu, \eta, \Delta, \epsilon, m)$. \diamond

4B. Classification. We have the following important theorem:

Theorem 4B.1. *Isomorphism classes of MTQFTs are in bijective correspondence with isomorphism classes of Möbius Frobenius algebras in $R\mathbf{Mod}$.*

Proof. First suppose that we are given a Möbius TQFT $\mathcal{F} : \mathbf{MCob} \rightarrow R\mathbf{Mod}$. If we define $V = \mathcal{F}(1)$, then it is clear that we can define R -linear maps $\mu_V = \mathcal{F}(\mu) : V \otimes V \rightarrow V$, $\eta_V = \mathcal{F}(\eta) : R \rightarrow V$, $\Delta_V = \mathcal{F}(\Delta) : V \rightarrow V \otimes V$, $\epsilon_V = \mathcal{F}(\epsilon) : V \rightarrow R$, and $m_V = \mathcal{F}(m) : V \rightarrow V$. From Remark 2A.16, it follows that $(V, \mu_V, \eta_V, \Delta_V, \epsilon_V)$ is a commutative Frobenius algebra in $R\mathbf{Mod}$ using the usual correspondence between oriented TQFTs and commutative Frobenius algebras. Furthermore, relations (2A.13) and (2A.15) ensure that m_V satisfies (4A.2) and (4A.3), and hence $(V, \mu_V, \eta_V, \Delta_V, \epsilon_V, m_V)$ is a Möbius Frobenius algebra in $R\mathbf{Mod}$. Finally, it is clear that given two Möbius TQFTs $\mathcal{F}, \mathcal{F}'$ and a symmetric monoidal natural isomorphism $\alpha : \mathcal{F} \rightarrow \mathcal{F}'$, the R -linear map $\alpha_1 : \mathcal{F}(1) \rightarrow \mathcal{F}'(1)$ is an isomorphism of Möbius Frobenius algebras in $R\mathbf{Mod}$.

Now suppose that we are given a Möbius Frobenius algebra $(V, \mu_V, \eta_V, \Delta_V, \epsilon_V, m_V)$ in $R\mathbf{Mod}$. Define a functor $\mathcal{F} : \mathbf{MCob} \rightarrow R\mathbf{Mod}$ by setting $\mathcal{F}(n) = V^{\otimes n}$ with $V^{\otimes 0} = R$ on objects. To define \mathcal{F} on morphisms, we refer to any given cobordism (or rather the corresponding isomorphism class of said cobordism) as a triple (S, B_I, B_F) with S a compact surface whose boundary is a disjoint union of two closed 1-manifolds $B_I = \bigsqcup_{i=1}^m \mathbb{S}^1$ and $B_F = \bigsqcup_{i=1}^m \mathbb{S}^1$ with fixed orientation. If S is orientable, then we can use the correspondence between oriented TQFTs and commutative Frobenius algebras to build a well-defined R -linear map $\mathcal{F}(S, B_I, B_F)$ using the corresponding generators $\mu_V, \eta_V, \Delta_V, \epsilon_V$ in place of $\mu, \eta, \Delta, \epsilon$ and relations (2A.3)–(2A.12).

Next consider the case that S is nonorientable i.e. there must be at least one m in any \circ - \otimes decomposition by generators. We then build $\mathcal{F}(S, B_I, B_F)$ exactly as in the oriented case, except with insertions of m_V whenever m appears in S . The resulting map is well-defined as usual, since m_V satisfies the same relations as m , together with their other respective generators.

Now we show that \mathcal{F} is indeed a functor, and that it is symmetric monoidal. The latter is clear. It is also clear that the identity cobordism is sent to the identity R -linear map on V . Furthermore, given two cobordisms $(S_1, (B_I)_1, (B_F)_1)$ and $(S_2, (B_I)_2, (B_F)_2)$ with $(B_F)_1 = (B_I)_2$, we can simply form the composite $(S_3, (B_I)_3, (B_F)_3) = (S_2 \circ S_1, (B_F)_2, (B_I)_1)$ much like the oriented case, since the boundaries have fixed orientations and are all copies of \mathbb{S}^1 i.e. all homeomorphisms between the boundaries must be trivial. By construction, it then follows that

$$\mathcal{F}(S_3, (B_I)_3, (B_F)_3) = \mathcal{F}(S_2, (B_I)_2, (B_F)_2) \circ \mathcal{F}(S_1, (B_I)_1, (B_F)_1)$$

as required.

In addition, it is a straightforward exercise to prove that if there exists an isomorphism of Möbius Frobenius algebras $f : V \rightarrow V'$, then there is a symmetric monoidal natural isomorphism $\alpha : \mathcal{F} \rightarrow \mathcal{F}'$.

Finally, it is clear that the two constructions above are inverses of one another. \square

Remark 4B.2. The proof of the above theorem is much simpler than the proof of a similar result for unoriented cobordisms e.g. in [TT06] primarily because of the fact that in our case the boundaries are all copies of \mathbb{S}^1 with fixed orientations, and so there are no nontrivial homeomorphisms between them. \diamond

Example 4B.3. Fix $R = \mathbb{Z}[\frac{1}{3}]$, and consider the MTQFT \mathcal{F} defined in Example 2B.3. We define the corresponding Möbius Frobenius algebra $(V, \mu_V, \eta_V, \Delta_V, \epsilon_V, m_V)$ by $V = \mathcal{F}(1)$, $\mu_V = \mathcal{F}(\mu)$, $\eta_V = \mathcal{F}(\eta)$, $\Delta_V = \mathcal{F}(\Delta)$, $\epsilon_V = \mathcal{F}(\epsilon)$, and $m_V = \mathcal{F}(m)$ as shown there. \diamond

We can translate the conditions on an MTQFT $\mathcal{F} : \mathbf{MCob} \rightarrow \mathbf{RMod}$ used to construct a chain complex and the Möbius homology of ribbon graphs from the previous section to the corresponding Möbius Frobenius algebra $(V, \mu_V, \eta_V, \Delta_V, \epsilon_V, m_V)$ as follows: we require that V is a finite-dimensional free \mathcal{G} -graded R -module whose R -linear maps μ_V , Δ_V , and m_V preserve the \mathcal{G} -grading up to the same constant shift, and that $m_V^2 = \mu_V \circ \Delta_V$. We can then build an identical chain complex with the R -module V together with the maps μ_V , Δ_V , and m_V . We will therefore work exclusively with Möbius Frobenius algebras going forward.

5. A CHOICE RELATED TO n -COLORING

We now explicitly construct a family of Möbius Frobenius algebras from which we define a ribbon graph invariant using the procedure outlined in Section 3C. We then compare the result to another known ribbon graph invariant, the *Penrose polynomial*, which has been the subject of much research (see e.g. [Aig97, EMM13] and, of course, [Pen71]) and whose evaluation at certain integral values relates to definitive properties of graphs e.g. the number of 3-edge colorings (or the number of 4-face colorings); we will see more examples at the end of this section.

5A. Möbius Frobenius algebras for the Penrose polynomial. Take $n \in \mathbb{N}_{>0}$, and set $R = \mathbb{Z}[\frac{1}{3n}]$. Consider the R -module

$$V = R[x, y]/(x^n, y^3 - xy).$$

We can immediately write down a basis $B = \{1, y, y^2, x, xy, xy^2, \dots, x^{n-1}, x^{n-1}y, x^{n-1}y^2\}$ of size $|B| = 3n$.

Now let $\mu_V : V \otimes V \rightarrow V$ be the usual multiplication map on the polynomial ring V , with $\eta_V : R \rightarrow V$, $r \mapsto r$ as the unit. Taking as the counit $\epsilon_V : V \rightarrow R$ with $\epsilon(x^{n-1}y^2) = 3n$ and zero on the other basis vectors, we have as the comultiplication $\Delta_V : V \rightarrow V \otimes V$:

$$(5A.1) \quad \begin{aligned} \Delta_V(v) = & -\frac{1}{3n} \sum_{\substack{i+j=n \\ i,j>0}} (v \cdot x^i) \otimes x^j \\ & + \frac{1}{3n} \sum_{i+j=n-1} (v \cdot x^i y^2) \otimes x^j + (v \cdot x^i y) \otimes x^j y + (v \cdot x^i) \otimes x^j y^2, \end{aligned}$$

for all $v \in V$. In other words, $(V, \mu_V, \eta_V, \Delta_V, \epsilon_V)$ is a commutative Frobenius algebra in \mathbf{RMod} . Furthermore, if we set

$$(5A.2) \quad m_V(v) = \begin{cases} v \cdot x^{(n-2)/2} y^2 & n \text{ even,} \\ v \cdot x^{(n-1)/2} y & n \text{ odd,} \end{cases}$$

for all $v \in V$, then (4A.2) is automatically satisfied. We also have that

$$(\mu_V \circ \Delta_V)(v) = v \cdot x^{n-1} y^2,$$

while

$$m_V^2(v) = \begin{cases} v \cdot x^{(n-2)/2} \cdot m_V(y^2) & n \text{ even,} \\ v \cdot x^{(n-1)/2} \cdot m_V(y) & n \text{ odd} \end{cases} = v \cdot x^{n-1} y^2 = (\mu_V \circ \Delta_V)(v),$$

which implies (4A.3). Therefore, we get the following.

Lemma 5A.3. *The above choices $(V, \mu_V, \eta_V, \Delta_V, \epsilon_V, m_V)$ give a Möbius Frobenius algebra in $R\mathbf{Mod}$.*

Proof. An easy calculation. \square

Example 5A.4. We have already seen the simplest case $n = 1$ in [Example 2B.3](#), so let us look at the simplest even case $n = 2$: firstly, we set $R = \mathbb{Z}[\frac{1}{6}]$. The base R -module is $V = R[x, y]/(x^2, y^3 - xy)$, which with respect to the basis $B = \{1, y, y^2, x, xy, xy^2\}$ has multiplication table

	1	y	y^2	x	xy	xy^2
1	1	y	y^2	x	xy	xy^2
y	y	y^2	xy	xy	xy^2	0
y^2	y^2	xy	xy^2	xy^2	0	0
x	x	xy	xy^2	0	0	0
xy	xy	xy^2	0	0	0	0
xy^2	xy^2	0	0	0	0	0

Given counit $\epsilon_V(xy^2) = 3 \cdot 2 = 6$ and zero otherwise, the pairing matrix is given by

$$\begin{pmatrix} 0 & 0 & 0 & 0 & 0 & 6 \\ 0 & 0 & 0 & 0 & 6 & 0 \\ 0 & 0 & 6 & 6 & 0 & 0 \\ 0 & 0 & 6 & 0 & 0 & 0 \\ 0 & 6 & 0 & 0 & 0 & 0 \\ 6 & 0 & 0 & 0 & 0 & 0 \end{pmatrix},$$

which has inverse

$$\frac{1}{6} \begin{pmatrix} 0 & 0 & 0 & 0 & 0 & 1 \\ 0 & 0 & 0 & 0 & 1 & 0 \\ 0 & 0 & 0 & 1 & 0 & 0 \\ 0 & 0 & 1 & -1 & 0 & 0 \\ 0 & 1 & 0 & 0 & 0 & 0 \\ 1 & 0 & 0 & 0 & 0 & 0 \end{pmatrix},$$

and so $\Delta_V(1) = -\frac{1}{6}x \otimes x + \frac{1}{6}(xy^2 \otimes 1 + xy \otimes y + x \otimes y^2 + y^2 \otimes x + y \otimes xy + 1 \otimes xy^2)$. Furthermore, we have $m_V(1) = y^2$, and so $m_V^2(1) = y^2 m_V(1) = y^4 = xy^2 = \mu_V(\Delta_V(1))$, where the first equality follows since $m_V(v) = v \cdot m_V(1)$ by construction for all $v \in V$. Therefore, for all $v \in V$, we have $m_V^2(v) = v \cdot m_V^2(1)$, and in addition, also by construction, $\mu_V(\Delta_V(v)) = v \cdot \mu_V(\Delta_V(1))$, and so we explicitly see that $m_V^2(v) = \mu_V(\Delta_V(v)) = (\mu_V \circ \Delta_V)(v)$. \diamond

At the end of [Section 4](#), we outlined the conditions that our Möbius Frobenius algebra given by $(V, \mu_V, \eta_V, \Delta_V, \epsilon_V, m_V)$ must satisfy in order to construct the Möbius homology of a given ribbon graph from [Section 3C](#). We already have that V is free and finite dimensional, and that $m_V^2 = \mu_V \circ \Delta_V$. We now need to specify a grading; for this, let

$$\mathcal{G} = \begin{cases} \mathbb{Z}/n\mathbb{Z} \times \mathbb{Z}/2\mathbb{Z} & n \text{ even,} \\ \mathbb{Z}/n\mathbb{Z} & n \text{ odd,} \end{cases}$$

and set $V = \bigoplus_{g \in \mathcal{G}} W_g$ such that

$$(5A.5) \quad x^i y^j \in \begin{cases} W_{(2i+j, j)} & n \text{ even,} \\ W_{2i+j} & n \text{ odd,} \end{cases}$$

where $0 \leq i \leq n-1$ and $0 \leq j \leq 2$.

Proposition 5A.6. *The \mathcal{G} -grading is well-defined for any element $x^i y^j$ in V with indices i, j defined over all nonnegative integers.*

Proof. We would like to establish that the \mathcal{G} -grading respects, in particular, the relations $x^n = 0$ and $y^3 = xy$ defining V . Let us begin by expressing any nonnegative integers i, j as $i = qn + r$ and $j = 3q' + r'$ with q, q' nonnegative integers, and $0 \leq r \leq n-1$, $0 \leq r' \leq 2$. We then have

$$(5A.7) \quad W_{(2i+j, j)} = W_{(2r+3q'+r', q'+r')} \quad \text{for } n \text{ even}$$

$$(5A.8) \quad W_{2i+j} = W_{2r+3q'+r'} \quad \text{for } n \text{ odd}$$

Note that, if $q > 0$, then $x^i y^j = 0$, which is in every graded subspace; in particular, the \mathcal{G} -grading respects the relation $x^n = 0$.

Furthermore, if $q' > 0$ and $q = 0$, we have $x^i y^j = x^r y^{3q'+r'} = x^{r+q'} y^{q'+r'}$ in V . We have

$$x^{r+q'} y^{q'+r'} \in \begin{cases} W_{(2r+2q'+q'+r', q'+r')} = W_{(2r+3q'+r', q'+r')} = W_{(2i+j, j)} & n \text{ even,} \\ W_{2r+2q'+q'+r'} = W_{2r+3q'+r'} = W_{2i+j} & n \text{ odd,} \end{cases}$$

where the final equality in both cases uses (5A.7) and (5A.8) respectively. The \mathcal{G} -grading therefore respects the relation $y^3 = xy$.

The remaining case i.e. $q = q' = 0$ is simply the base case covered in (5A.5). \square

Example 5A.9. For $n = 1$, the grading is trivial. For $n = 2$, we have the following decomposition $V = W_{(0,0)} \oplus W_{(1,0)} \oplus W_{(0,1)} \oplus W_{(1,1)}$ with $1, y^2, x, xy^2 \in W_{(0,0)}$ and $y, xy \in W_{(1,1)}$, with $W_{(1,0)} = W_{(0,1)} = \{0\}$. \diamond

Proposition 5A.10. *The maps μ_V , Δ_V , and m_V preserve the \mathcal{G} -grading with zero shift.*

Proof. First, observe that $x^i y^j \cdot x^{i'} y^{j'} = x^{i+i'} y^{j+j'}$ with

$$x^{i+i'} y^{j+j'} \in \begin{cases} W_{(2i+2i'+j+j', j+j')} = W_{(2i+j, j)+(2i'+j', j')} & n \text{ even,} \\ W_{2i+2i'+j+j'} = W_{(2i+j)+(2i'+j')} & n \text{ odd,} \end{cases}$$

where we have used Proposition 5A.6 to define the \mathcal{G} -grading for any nonnegative i, i', j, j' , which shows that μ_V preserves the \mathcal{G} -grading with zero shift.

Now suppose that we are given a $v \in V$ such that $v \in W_g$ for some $g \in \mathcal{G}$. From the definition (5A.1) of comultiplication, the first summation in $\Delta_V(v)$ contains terms with \mathcal{G} -grading $g + (2i, 0) + (2j, 0) = g + (2(i+j), 0) = g + (2n, 0) = g + (0, 0) = g$ for n even, and an analogous computation for n odd. Similarly, the second summation contains terms with \mathcal{G} -grading $g + (2(i+j) + 2, 2) = g + (2(n-1) + 2, 0) = g + (2n, 0) = g + (0, 0) = g$ for n even, and an analogous computation for n odd. Therefore, Δ_V preserves the \mathcal{G} -grading with zero shift.

Finally, from the definition (5A.2), the element $m_V(v)$ has \mathcal{G} -grading $g + (2(n-2)/2 + 2, 2) = g + (n, 0) = g + (0, 0) = g$ for n even, and $g + 2(n-1)/2 + 1 = g + n = g$ for n odd. Therefore, m_V also preserves the \mathcal{G} -grading with zero shift, and the proposition is proven. \square

We can now build a chain complex and Möbius homology associated with the specified Möbius Frobenius algebra $(V, \mu_V, \eta_V, \Delta_V, \epsilon_V, m_V)$ of any ribbon graph. From here, it is straightforward to determine the graded Euler characteristic by first calculating the graded dimension of V . As before in Example 3C.1, we use the grading variables q and b .

Proposition 5A.11. *The graded dimension of V is given by:*

$$qdim(V) = \begin{cases} 2(2 + 2q^2 + \dots + 2q^{n-2} + qb + \dots + q^{n-1}b) & n \text{ even,} \\ 3(1 + q + \dots + q^{n-1}) & n \text{ odd.} \end{cases}$$

Proof. For n even, $\mathcal{G} = \mathbb{Z}/n\mathbb{Z} \times \mathbb{Z}/2\mathbb{Z}$ with two associated generators, and so the graded dimension is a polynomial in two variables, say q, b . As the integer i runs from 0 to $n-1$, it follows that $2i \bmod n$ coming from the grading of x^i , as well as $2i + 2 \bmod n$ coming from the grading of $x^i y^2$, hits all the even integers from 0 to $n-2$ twice. On the other hand, $2i + 1 \bmod n$, coming from the grading of $x^i y$, hits all the odd integers from 1 to $n-1$ twice. Therefore, $W_{(2i,0)}$ are four dimensional while $W_{(2i+1,1)}$ are two dimensional given $i = 0, \dots, n/2 - 1$.

For n odd, $\mathcal{G} = \mathbb{Z}/n\mathbb{Z}$ with one associated generator, and so the graded dimension is a polynomial in one variable, say q . As the integer i runs from 0 to $n-1$, it is straightforward to see that $2i \bmod n$ coming from the grading of x^i , $2i + 2 \bmod n$ coming from the grading of $x^i y^2$, and $2i + 1 \bmod n$ coming from the grading of $x^i y$, each hit all integers from 0 to $n-1$. Therefore, each $W_g, g \in \mathbb{Z}/n\mathbb{Z}$, is three dimensional. \square

Example 5A.12. Following from Example 2B.3 and Example 5A.9, we know that for $n = 1$ the grading is trivial and there are three basis vectors, and so $qdim(V) = 3$, as expected. For $n = 2$, from Example 5A.9 we know that there are four basis vectors with grading $(0, 0)$ and the remaining two basis vectors have grading $(1, 1)$, giving $qdim(V) = 4 + 2qb$, also as expected. \diamond

Given a perfect matching graph Γ_M with trivalent underlying graph G , which is trivalent with perfect matching M , we can then determine the graded Euler characteristic using Theorem 3C.17 together with Proposition 5A.11: we simply calculate the bracket $\langle \Gamma_M \rangle_n$ of Γ_M characterized by the following skein relations:

$$(5A.13) \quad \left\langle \begin{array}{c} \diagup \quad \diagdown \\ \bullet \quad \bullet \\ \vdots \\ \bullet \quad \bullet \\ \diagdown \quad \diagup \end{array} \right\rangle_n = \left\langle \begin{array}{c} | \quad | \\ | \quad | \end{array} \right\rangle_n - \left\langle \begin{array}{c} \diagup \quad \diagdown \\ \diagdown \quad \diagup \end{array} \right\rangle_n,$$

$$(5A.14) \quad \left\langle \bigcirc \right\rangle_n = \begin{cases} 2(2 + 2q^2 + \dots + 2q^{n-2} + qb + \dots + q^{n-1}b) & n \text{ even,} \\ 3(1 + q + \dots + q^{n-1}) & n \text{ odd,} \end{cases}$$

$$(5A.15) \quad \langle \Gamma_1 \sqcup \Gamma_2 \rangle_n = \langle \Gamma_1 \rangle_n \cdot \langle \Gamma_2 \rangle_n.$$

We think of (5A.13)–(5A.15) as a refinement of (3B.2)–(3B.4).

We can also write down the associated graded Poincaré polynomial, defined in (3C.18), and we will see explicit examples of this in Section 6.

Remark 5A.16. Note that setting $t = -1$ in the graded Poincaré polynomial also gives the graded Euler characteristic (see the proof of the second part of Theorem 3C.17). \diamond

5B. Penrose polynomial. Suppose that we are given a ribbon graph Γ and associated blowup Γ^b . Now use the canonical perfect matching of Γ^b , with the edges of the underlying graph of Γ as the perfect matching, to form the perfect matching graph Γ_E^b . The Penrose polynomial $P(\Gamma, n)$ of Γ is then the bracket $\langle \Gamma_E^b \rangle$ from Definition 3B.1 with $A = 1$, $B = -1$, and $C = n$. Using Remark 3B.6, Proposition 3B.7 and the rest of the discussion in Section 3B, we can conclude that $P(\Gamma, n)$ is indeed a well-defined ribbon graph invariant.

Let $\langle \Gamma_E^b \rangle_n$ denote the bracket associated with the Möbius homology characterized by (5A.13)–(5A.15) above. We have the following proposition.

Proposition 5B.1. *Recall that as a polynomial, $\langle \Gamma_E^b \rangle_n = \langle \Gamma_E^b \rangle_n(q, b)$ for n even and for n odd, $\langle \Gamma_E^b \rangle_n = \langle \Gamma_E^b \rangle_n(q)$. We have that:*

$$\langle \Gamma_E^b \rangle_n(q, b) = \begin{cases} P(\Gamma, 3n) & \text{when } q = b = 1, \\ P(\Gamma, n) & \text{when } q = 1, b = -1, \end{cases}$$

for n even, and

$$\langle \Gamma_E^b \rangle_n(1) = P(\Gamma, 3n)$$

for n odd.

Proof. In (5A.14), for n even, if we set $q = b = 1$,

$$(5B.2) \quad 2(2 + 2q^2 + \dots + 2q^{n-2} + qb + \dots + q^{n-1}b) = \begin{cases} 2(2n/2 + n/2) = 3n & q = b = 1, \\ 2(2n/2 - n/2) = n & q = 1, b = -1, \end{cases}$$

and since n is even, $(qb)^n = 1$ and b only appears with odd powers of q i.e. setting $q = 1$, $b = -1$ before or after taking powers of the l.h.s. of (5B.2) does not affect the computation; of course this is also trivially true for $q = b = 1$.

For n odd, setting $q = 1$ gives

$$(5B.3) \quad 3(1 + q + \dots + q^{n-1}) = 3n,$$

and setting $q = 1$ before or after taking powers of the l.h.s. of (5B.3) again does not affect the computation.

Altogether, we have shown that the skein relations characterizing the Penrose polynomial have been recovered for the respective cases. \square

We conclude this section by listing some of the explicit ribbon graph invariants that can be obtained using the Penrose polynomial; for more information and proofs, see [Aig97, EMM13, Pen71].

For the Möbius Frobenius algebra from Section 5, write

$$MH_n^{i,g}(\Gamma_M; R) \text{ and } Mh_n(\Gamma_M)$$

for the corresponding Möbius homology and graded Poincaré polynomial, respectively. For n even, write $g = (a, \epsilon) \in \mathbb{Z}/n\mathbb{Z} \times \mathbb{Z}/2\mathbb{Z}$.

Definition 5B.4. For n even, define the *positive and negative parts of the Möbius homology* and their q -graded ranks by

$$MH_n^+(\Gamma_M; R) = \bigoplus_{\substack{i, a, \epsilon \\ i + \epsilon \equiv 0 \pmod{2}}} MH_n^{i, (a, \epsilon)}(\Gamma_M; R), \quad Q_n^+(\Gamma_M) = q \dim MH_n^+(\Gamma_M; R)|_{b=1},$$

$$MH_n^-(\Gamma_M; R) = \bigoplus_{\substack{i, a, \epsilon \\ i + \epsilon \equiv 1 \pmod{2}}} MH_n^{i, (a, \epsilon)}(\Gamma_M; R) \quad Q_n^-(\Gamma_M) = q \dim MH_n^-(\Gamma_M; R)|_{b=1},$$

where we set $b = 1$. Moreover, for $f, g \in \mathbb{Z}[q]/(q^4 - 1)$, write $f >_{\text{cw}} g$ if, after representing $f - g$ as $c_0 + c_1q + c_2q^2 + c_3q^3$, all coefficients c_i are nonnegative and at least one is positive. \diamond

For simplicity of notation, in the final point of [Theorem 5B.5](#), the numbers n' and x are determined by [Proposition 5B.1](#).

Theorem 5B.5. *Let Γ be a ribbon graph whose underlying graph $G = (V, E, r)$ is connected and planar. We have the following:*

- (a) $\langle \Gamma_E^b \rangle_2(1, -1) = 2^{|V|}$ if Γ is Eulerian and zero otherwise.
- (b) $\langle \Gamma_E^b \rangle_1(1) = \#\{3\text{-edge colorings of } \Gamma\}$ when Γ is trivalent.
- (c) Γ is 4-face colorable if and only if

$$(Q_4^+(\Gamma_E^b) - Q_4^-(\Gamma_E^b))|_{q=1} > 0.$$

In particular, the q -graded homological condition

$$Q_4^+(\Gamma_E^b) >_{\text{cw}} Q_4^-(\Gamma_E^b)$$

implies that Γ is 4-face colorable. Thus proving this coefficientwise positivity condition for every connected planar ribbon graph Γ would imply the four color theorem.

- (d) Given a nonnegative integer n with $n \in 2\mathbb{Z}$ or $n \in 3\mathbb{Z}$, $\langle \Gamma_E^b \rangle_n(x) \geq \chi(\Gamma^*, n')$, where $\chi(\Gamma^*, n')$ is the chromatic polynomial of the geometric dual of Γ .

Proof. The polynomial statements follow from [Proposition 5B.1](#) and certain facts about the Penrose polynomial, cf. [[Aig97](#), [EMM13](#), [Pen71](#)]. For part (c), [Theorem 3C.17](#) gives

$$Q_4^+(\Gamma_E^b) - Q_4^-(\Gamma_E^b) = Mh_4(\Gamma_E^b)|_{t=-1, b=-1}.$$

Therefore,

$$(Q_4^+(\Gamma_E^b) - Q_4^-(\Gamma_E^b))|_{q=1} = Mh_4(\Gamma_E^b)|_{t=-1, q=1, b=-1} = \langle \Gamma_E^b \rangle_4(1, -1).$$

By [Proposition 5B.1](#), the final expression is $P(\Gamma, 4)$, and the Penrose polynomial statement says that $P(\Gamma, 4) > 0$ if and only if Γ is 4-face colorable. This proves the equivalence. Finally, if $Q_4^+(\Gamma_E^b) >_{\text{cw}} Q_4^-(\Gamma_E^b)$, then evaluating at $q = 1$ gives a positive integer, so Γ is 4-face colorable. \square

Remark 5B.6. There are other results for n negative, however these ranges of n cannot be reached in our construction so we omit them. In the case $n = 0$, though not explicitly included, we can simply define $\langle \Gamma_E^b \rangle_0(1, -1) = 0 = P(\Gamma, 0)$. \diamond

Remark 5B.7. We point out that [Theorem 5B.5](#)(c) is in the same general spirit as several approaches to the four color theorem via graph and web homologies.

Firstly, Baldridge [[Bal18](#)] constructed a cohomology theory for planar trivalent graphs with perfect matchings whose graded Euler characteristic detects even perfect matchings, and therefore gives a homological route to four-face colorability. Baldridge–McCarty [[BM23](#)] later constructed TQFT-type homologies whose dimensions encode face colorings of cell decompositions of surfaces, leading to a constructive homological approach to four-face coloring.

There is also a closely related web-and-foam viewpoint. Kronheimer–Mrowka [[KM19](#)] introduced an instanton homology for webs and foams, with a nonvanishing theorem motivated by a possible new proof of the four color theorem. Khovanov–Robert [[KR21](#)] then constructed combinatorial foam-evaluation analogs of these Kronheimer–Mrowka theories for planar trivalent graphs. \diamond

6. EXAMPLES AND COMPUTER TALK

We now give a few calculation examples.

0	$\begin{aligned} &< 1 \otimes y - y \otimes 1, \\ &y \otimes y^2, y^2 \otimes y, y^2 \otimes y^2, \\ &y \otimes y - 1 \otimes y^2, \\ &y^2 \otimes 1 - 1 \otimes y^2 > \end{aligned}$	0
j / i	0	1

 TABLE 1. Möbius homology for E_1 , $n = 1$.

(1, 1)	$\begin{aligned} &< x \otimes xy, xy \otimes x, 1 \otimes xy - xy \otimes 1, \\ &x \otimes y - y \otimes x, \\ &xy \otimes xy^2, xy^2 \otimes xy, y^2 \otimes xy, \\ &xy \otimes y^2, 1 \otimes y - y \otimes 1, \\ &y \otimes xy^2, xy^2 \otimes y, y \otimes y^2 - y^2 \otimes y, \\ &x \otimes y - y \otimes y^2, x \otimes y - 1 \otimes xy > \end{aligned}$	0
(0, 0)	$\begin{aligned} &< xy \otimes xy, xy^2 \otimes xy^2, x \otimes xy^2, xy^2 \otimes x, \\ &x \otimes x, xy^2 \otimes y^2, y^2 \otimes xy^2, 1 \otimes x - x \otimes 1, \\ &1 \otimes y^2 - y^2 \otimes 1, 1 \otimes xy^2 - xy^2 \otimes 1, \\ &x \otimes y^2 - 1 \otimes xy^2, \\ &y^2 \otimes x - 1 \otimes xy^2, y \otimes xy - 1 \otimes xy^2, \\ &xy \otimes y - 1 \otimes xy^2, \\ &y \otimes y - 1 \otimes y^2, y^2 \otimes y^2 - 1 \otimes xy^2 > \end{aligned}$	0
j / i	0	1

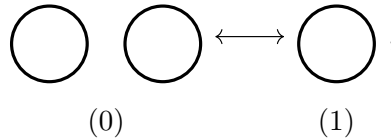
 TABLE 2. Möbius homology for E_1 , $n = 2$.

6A. By hand calculations. We begin this section by computing the graded Poincaré polynomial associated with the Möbius homology outlined in the previous sections for three explicit examples of perfect matching graphs: E_1 , E_2 , and E_3 shown in [Example 3A.15](#). We will concentrate on the cases $n = 1, 2$, the simplest examples of n odd and even respectively.

Example 6A.1. The hypercube of states corresponding to the perfect matching graph



is given by



and so we can write our complex generically as

$$\begin{array}{ccc}
 V \otimes V & \xrightarrow{\mu_V} & V \\
 & & \phantom{\xrightarrow{\mu_V}} \\
 i = 0 & & i = 1
 \end{array}$$

with $V = R[x, y]/(x^n, y^3 - xy)$ and μ_V given by multiplication on the polynomial ring V as discussed in the previous section.

For $n = 1$, the grading is trivial, and since $\text{rank}(\mu_V) = \dim(V) = 3$, $\text{null}(\mu_V) = 9 - 3 = 6$. The resulting homology is show in [Table 1](#); therefore, we have that $Mh(E_1) = 6$.

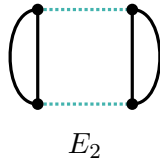
For $n = 2$, we have $\mathcal{G} = \mathbb{Z}/2\mathbb{Z} \times \mathbb{Z}/2\mathbb{Z}$ and all elements of V are spread over the gradings (0, 0) and (1, 1). Since $\text{rank}(\mu_V) = \dim(V) = 6$, $\text{null}(\mu_V) = 36 - 6 = 30$ spread over gradings (0, 0) and

0	$\langle y \otimes y^2, y^2 \otimes y, y^2 \otimes y^2, \\ 1 \otimes y - y \otimes 1, y \otimes y - 1 \otimes y^2, \\ y^2 \otimes 1 - 1 \otimes y^2 \rangle$	0	$\langle 1 \otimes 1, 1 \otimes y^2, y \otimes y, \\ y^2 \otimes 1, y \otimes y^2, \\ y^2 \otimes y \rangle$
j i	0	1	2

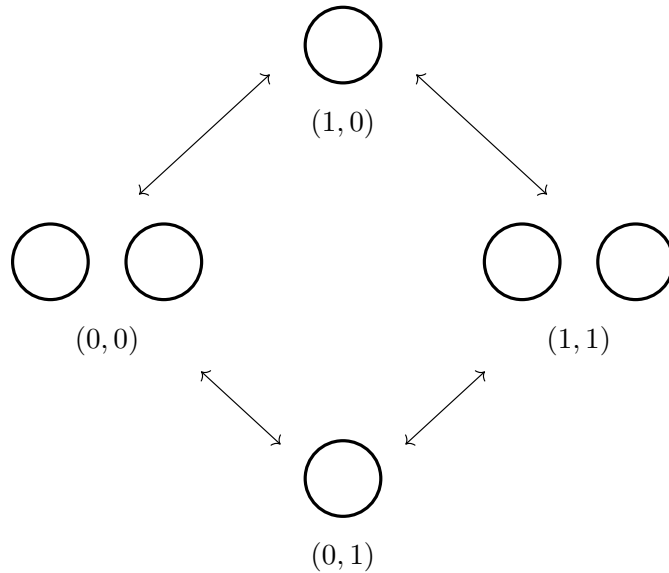
TABLE 3. Möbius homology for E_2 , $n = 1$.

(1, 1). Enumerating over all possibilities gives the homology shown in Table 2, and so we have that $Mh(E_1) = 16 + 14qb$. Furthermore, notice that E_1 is the blowup of a ribbon graph with one vertex and one edge with the canonical perfect matching; using Proposition 5B.1 and Theorem 5B.5, we see that $16 + 14(1)(-1) = 2 = 2^1$, as expected. \diamond

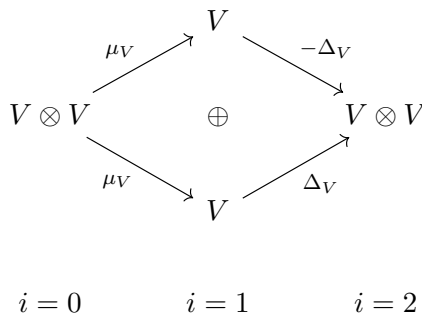
Example 6A.2. The hypercube of states corresponding to the perfect matching graph



is given by



with corresponding complex



as shown in Example 3B.8 and Example 3C.7, except that we have included signs for the maps in the complex as required in the definition of the differential. Aside from the multiplication map μ_V , we see the comultiplication Δ_V , which is defined by (5A.1).

For $n = 1$, in particular for comultiplication, the explicit maps are given in Example 2B.3. The $i = 0$ homology is already given in Table 1. Given $\partial^1(v, v') : V \oplus V \rightarrow V \otimes V$, $(v, v') \mapsto -\Delta_V(v) + \Delta_V(v')$ and since $\text{rank}(\Delta_V) = 3$, $\text{null}(\partial^1) = 3$ and so the $i = 1$ homology is 0. For $i = 2$, we have

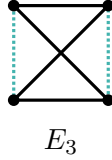
(1, 1)	$\langle x \otimes xy, xy \otimes x, 1 \otimes xy - xy \otimes 1, x \otimes y - y \otimes x, xy \otimes xy^2, xy^2 \otimes xy, y^2 \otimes xy, xy \otimes y^2, 1 \otimes y - y \otimes 1, y \otimes xy^2, xy^2 \otimes y, y \otimes y^2 - y^2 \otimes y, x \otimes y - y \otimes y^2, x \otimes y - 1 \otimes xy \rangle$	0	$\langle 1 \otimes y, 1 \otimes xy, x \otimes y, x \otimes xy, y \otimes 1, y \otimes x, y \otimes y^2, y^2 \otimes y, xy \otimes 1, xy \otimes x, y \otimes xy^2, y^2 \otimes xy, xy \otimes y^2, xy \otimes xy^2 \rangle$
(0, 0)	$\langle xy \otimes xy, xy^2 \otimes xy^2, x \otimes xy^2, xy^2 \otimes x, x \otimes x, xy^2 \otimes y^2, y^2 \otimes xy^2, 1 \otimes x - x \otimes 1, 1 \otimes y^2 - y^2 \otimes 1, 1 \otimes xy^2 - xy^2 \otimes 1, x \otimes y^2 - 1 \otimes xy^2, y^2 \otimes x - 1 \otimes xy^2, y \otimes xy - 1 \otimes xy^2, xy \otimes y - 1 \otimes xy^2, y \otimes y - 1 \otimes y^2, y^2 \otimes y^2 - 1 \otimes xy^2 \rangle$	0	$\langle 1 \otimes 1, 1 \otimes x, 1 \otimes y^2, x \otimes 1, y \otimes y, y^2 \otimes 1, y^2 \otimes y^2, 1 \otimes xy^2, x \otimes x, x \otimes y^2, y \otimes xy, y^2 \otimes x, xy \otimes y, x \otimes xy^2, xy \otimes xy, y^2 \otimes xy^2 \rangle$
$\begin{array}{c} j \\ \hline i \end{array}$	0	1	2

 TABLE 4. Möbius homology for E_2 , $n = 2$.

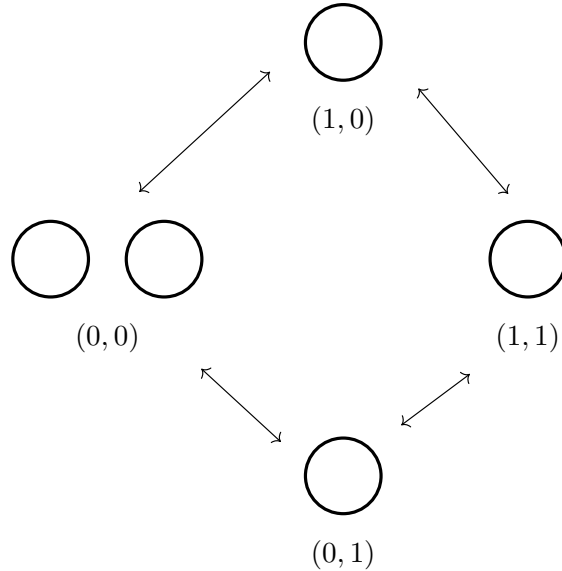
$\text{rank}(\partial^1) = 6 - 3 = 3$ and since the nullity of the final zero map is $3 \cdot 3 = 9$, the dimension of the $i = 2$ homology is $9 - 3 = 6$ with basis given in Table 3. Therefore, $Mh(E_2) = 6 + 6t^2$.

For $n = 2$, the explicit maps (evaluated on 1) are given in Example 5A.4. The $i = 0$ homology is again already given in Table 2. By a similar reasoning to the $n = 1$ case, with now $\text{rank}(\Delta_V) = 6$, the $i = 1$ homology is 0, and the dimension of the $i = 2$ homology is $6 \cdot 6 - 6 = 36 - 6 = 30$ with basis, spread over $(0, 0)$ and $(1, 1)$, given in Table 4. Therefore, $Mh(E_2) = 16 + 14qb + 16t^2 + 14qbt^2$. Furthermore, notice that E_2 is the blowup of a ribbon graph with two vertices and two edges between the vertices, with the canonical perfect matching; using Proposition 5B.1 and Theorem 5B.5, we see that $16 + 14(1)(-1) + 16(-1)^2 + 14(1)(-1)(-1)^2 = 4 = 2^2$, as expected. \diamond

Example 6A.3. The hypercube of states corresponding to the perfect matching graph



is given by



characteristic associated with the Möbius homology, for E_1 is $q\dim(V)^2 - q\dim(V)$, which is the same as

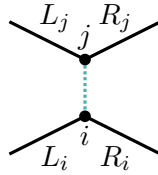
$$q\dim(V)^2 - 2q\dim(V) + q\dim(V) = q\dim(V)^2 - q\dim(V)$$

for E_2 , where $V = R[x, y]/(x^n, y^3 - xy)$ is the Möbius Frobenius algebra from Section 5 with n a positive integer.

On the other hand, since the multiplication map μ_V is obviously full rank, the homology group of homological degree $i = 1$ for E_1 is 0 for all positive integers n i.e. the graded Poincaré polynomial for E_1 given by (3C.18) contains no nontrivial powers of t . For E_3 , however, the degree $i = 2$ homology group contains at least $\langle 1 \rangle$ for all positive integers n since the map m_V , given in (5A.2), is not full rank; in particular, neither y nor y^2 is invertible in V . Therefore, the graded Poincaré polynomial for E_3 contains a nonzero coefficient of t^2 , and the result is proved. \square

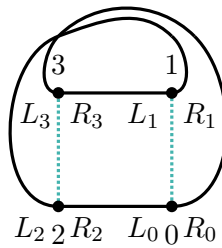
6B. Computer talk. For the remainder of this section, we briefly describe some Python code for producing the Poincaré polynomial as shown in Example 6A.1, Example 6A.2, and Example 6A.3 above, but now for general perfect matching graphs. For further details and code files, we direct the reader to [CT26a].

Our input is a perfect matching graph Γ_M , whose underlying graph $G = (V, E, r)$ is trivalent with perfect matching M . The vertices are encoded as points $\{0, 1, \dots, |V| - 1\}$, and perfect matching edges are specified as (unordered) pairs of points. To specify the remaining edges, for each vertex $i = 0, 1, \dots, |V| - 1$ in order, associate an ordered pair of vertices (v_i, w_i) for which there are edges L_i and R_i , away from the perfect matching edge, with $L_i = \{i, v_i\}$ and $R_i = \{i, w_i\}$. By convention, the ordering (v_i, w_i) is determined by forming an equivalent perfect matching graph where the perfect matchings locally have the following fixed configuration:



with $j > i$; such a configuration is always possible at every vertex since G is trivalent and every vertex is adjacent to a perfect matching, by definition of a perfect matching.

For example, we can input the perfect matching graph E_3 from Example 3A.15 as follows, together with the accompanying illustration:



```
pairs = [[2, 3], [3, 2], [1, 0], [0, 1]]
matching = [[0, 1], [2, 3]]
```

The final input is the positive integer n , which fixes the choice of Möbius Frobenius algebra $V = R[x, y]/(x^n, y^3 - xy)$ specified in Section 5. For purposes of the code, we set $R = \mathbb{Q}$. For example, we could look at the simplest case $n = 1$ i.e. $V = \mathbb{Q}[y]/(y^3)$:

```
n = 1
```

We can now run the code, for example:

```
MH = MobiusHomology(pairs, matching, n=n)
```

The essential functions performed are as follows:

- (i) Construction of the hypercube of states returned as a list of lists giving the number of circles in each state of fixed $|\alpha|$, which is later interpreted as the homological degree. The code also

keeps track of which circles change when moving along a directed edge in order to later assign the μ_V , Δ_V , and m_V maps to the correct tensor power in the chain complex.

In our example, we can run

```
print('circle counts by homological degree:', MH.state_circle_counts())
```

The output is

```
circle counts by homological degree: [[2], [1, 1], [1]]
```

as expected.

- (ii) Computation of the differential defined in (3C.13) at each homological degree, which can be viewed as a matrix if desired by running, for example at degree 0:

```
degree = 0
D = MH.differential_matrix(degree)
print('shape:', D.shape)
D
```

which outputs both the shape of the matrix and the matrix itself.

- (iii) Extraction of the dimension of the homology groups at each homological degree by standard rank-nullity linear algebra. For the total dimensions, we can run:

```
print('homology dimensions by homological degree:', MH.homology_dimensions())
```

which returns

```
homology dimensions by homological degree: [6, 1, 1]
```

as expected from Table 5. For the dimensions listed by grading, we can run:

```
print('homology dimensions by internal degree:', MH.
      homology_dimensions_by_internal_degree())
```

which returns

```
homology dimensions by internal degree: {0: [6, 1, 1]}
```

also as expected; recall that for $n = 1$, the grading is trivial.

- (iv) Formation of the graded Poincaré polynomial by running:

```
print('Poincare polynomial:', MH.poincare_polynomial())
```

which returns

```
Poincare polynomial: t**2 + t + 6
```

as expected for our example.

- (v) A final check that $\partial^2 = 0$ by running:

```
print('d^2 = 0:', MH.check_d_squared())
```

which returns a Boolean

```
d^2 = 0: True
```

as required.

Remark 6B.1. For n even, we have chosen to ignore the $\mathbb{Z}/2\mathbb{Z}$ component in the grading $\mathcal{G} = (\mathbb{Z}/n\mathbb{Z}, \mathbb{Z}/2\mathbb{Z})$ in the code for convenience: only a single q variable for the grading appears in the graded Poincaré polynomial. Of course, by replacing q^i with $q^i b$ for i odd in the final result, the $\mathbb{Z}/2\mathbb{Z}$ component can be restored. \diamond

We conclude this section with a few more examples.

Example 6B.2. We run the code again on E_3 , but for higher n . For $n = 3$, the output is

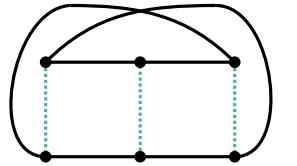
```
circle counts by homological degree: [[2], [1, 1], [1]]
d^2 = 0: True
homology dimensions by homological degree: [72, 5, 5]
homology dimensions by internal degree: {0: [24, 1, 1], 1: [24, 2, 2], 2: [24, 2,
2]}
Poincare polynomial: 2*q**2*t**2 + 2*q**2*t + 24*q**2 + 2*q*t**2 + 2*q*t + 24*q + t
**2 + t + 24
```

and for $n = 4$,

```
circle counts by homological degree: [[2], [1, 1], [1]]
d^2 = 0: True
homology dimensions by homological degree: [132, 7, 7]
homology dimensions by internal degree: {0: [36, 2, 2], 1: [30, 1, 1], 2: [36, 3, 3], 3: [30, 1, 1]}
Poincare polynomial: q**3*t**2 + q**3*t + 30*q**3 + 3*q**2*t**2 + 3*q**2*t + 36*q**2 + q*t**2 + q*t + 30*q + 2*t**2 + 2*t + 36
```

Notice that the total homology dimensions appear to follow the pattern $(3n)^2 - 3n$, $2n - 1$, and $2n - 1$ for $i = 0, 1$, and 2 respectively. In general, the result holds by standard rank-nullity analysis for the maps μ_V and m_V , which we will not do here. \diamond

Example 6B.3. Consider the following perfect matching graph:



also known as $K_{3,3}$, with the additional perfect matching specified. We can input $K_{3,3}$ as

```
pairs = [[5, 3], [2, 4], [3, 1], [0, 2], [1, 5], [4, 0]]
matching = [[0, 1], [5, 2], [4, 3]]
```

which outputs

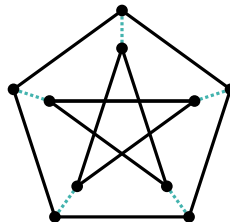
```
circle counts by homological degree: [[3], [2, 2, 2], [1, 1, 1], [2]]
d^2 = 0: True
homology dimensions by homological degree: [8, 2, 0, 6]
homology dimensions by internal degree: {0: [8, 2, 0, 6]}
Poincare polynomial: 6*t**3 + 2*t + 8
```

for $n = 1$, and for $n = 2$:

```
circle counts by homological degree: [[3], [2, 2, 2], [1, 1, 1], [2]]
d^2 = 0: True
homology dimensions by homological degree: [126, 6, 0, 30]
homology dimensions by internal degree: {0: [63, 3, 0, 16], 1: [63, 3, 0, 14]}
Poincare polynomial: 14*q*t**3 + 3*q*t + 63*q + 16*t**3 + 3*t + 63
```

Note that we could take $K_{3,3}$ without the specified perfect matching and consider the blowup with the canonical perfect matching instead, though the resulting perfect matching graph would of course be much more complicated. \diamond

Example 6B.4. Finally, consider the Petersen graph with following perfect matching:



where the input may be given as:

```
pairs = [[4, 1], [0, 2], [1, 3], [2, 4], [3, 0], [8, 7], [9, 8], [5, 9], [6, 5], [7, 6]]
matching = [[0, 5], [1, 6], [2, 7], [3, 8], [4, 9]]
```

The output is

```
circle counts by homological degree: [[1], [1, 1, 1, 1, 1], [2, 1, 1, 2, 2, 1, 1, 2, 1, 2], [1, 2, 1, 2, 2, 1, 1, 2, 2, 1], [1, 1, 1, 1, 1], [1]]
d^2 = 0: True
homology dimensions by homological degree: [1, 1, 8, 8, 1, 1]
```

```

homology dimensions by internal degree: {0: [1, 1, 8, 8, 1, 1]}
Poincare polynomial: t**5 + t**4 + 8*t**3 + 8*t**2 + t + 1

circle counts by homological degree: [[1], [1, 1, 1, 1, 1], [2, 1, 1, 2, 2, 1, 1, 2,
1, 2], [1, 2, 1, 2, 2, 1, 1, 2, 2, 1], [1, 1, 1, 1, 1], [1]]
d^2 = 0: True
homology dimensions by homological degree: [3, 3, 66, 66, 3, 3]
homology dimensions by internal degree: {0: [2, 2, 34, 34, 2, 2], 1: [1, 1, 32, 32,
1, 1]}
Poincare polynomial: q*t**5 + q*t**4 + 32*q*t**3 + 32*q*t**2 + q*t + q + 2*t**5 + 2*
t**4 + 34*t**3 + 34*t**2 + 2*t + 2

```

for $n = 1, 2$ respectively. Note that the homology here is much stronger at its decategorification at $t = -1$, since the latter vanishes. \diamond

REFERENCES

- [Aig97] M. Aigner. The Penrose polynomial of a plane graph. *Math. Ann.*, 307:173–189, 1997. doi:10.1007/s002080050030.
- [Bal18] S. Baldrige. A cohomology theory for planar trivalent graphs with perfect matchings. Preprint, 2018. <https://arxiv.org/abs/1810.07302>, doi:10.48550/arXiv.1810.07302.
- [BKM22] S. Baldrige, L. H. Kauffman, and B. McCarty. Unoriented virtual Khovanov homology. *New York J. Math.*, 28:367–401, 2022. <https://arxiv.org/abs/2001.04512>.
- [BKR22] S. Baldrige, L. H. Kauffman, and W. Rushworth. On ribbon graphs and virtual links. *European J. Combin.*, 103:103520, 2022. <https://arxiv.org/abs/2010.04238>, doi:10.1016/j.ejc.2022.103520.
- [BM23] S. Baldrige and B. McCarty. A topological quantum field theory approach to graph coloring. 2023. <https://arxiv.org/abs/2303.12010>.
- [BN97] D. Bar-Natan. Lie algebras and the Four Color Theorem. *Combinatorica*, 17(1):43–52, 1997. <https://arxiv.org/abs/q-alg/9606016>, doi:10.1007/BF01196130.
- [BN05] D. Bar-Natan. Khovanov’s homology for tangles and cobordisms. *Geom. Topol.*, 9:1443–1499, 2005. <https://arxiv.org/abs/math/0410495>, doi:10.2140/gt.2005.9.1443.
- [BHMV95] C. Blanchet, N. Habegger, G. Masbaum, and P. Vogel. Topological quantum field theories derived from the Kauffman bracket. *Topology*, 34(4):883–927, 1995. doi:10.1016/0040-9383(94)00051-4.
- [BR02] B. Bollobás and O. Riordan. A polynomial of graphs on surfaces. *Math. Ann.*, 323(1):81–96, 2002. doi:10.1007/s002080100297.
- [Chm09] S. Chmutov. Generalized duality for graphs on surfaces and the signed Bollobás–Riordan polynomial. *J. Combin. Theory Ser. B*, 99(3):617–638, 2009. <https://arxiv.org/abs/0711.3490>, doi:10.1016/j.jctb.2008.09.007.
- [CMW09] D. Clark, S. Morrison, and K. Walker. Fixing the functoriality of Khovanov homology. *Geom. Topol.*, 13(3):1499–1582, 2009. <https://arxiv.org/abs/math/0701339>, doi:10.2140/gt.2009.13.1499.
- [CT26a] D. W. Collison and D. Tubbenhauer. Code, data and more for “Categorification of some Penrose polynomials”. 2026. <https://github.com/dtubbenhauer/graphhomology>.
- [CT26b] D. W. Collison and D. Tubbenhauer. Möbius strip diagram algebras. 2026. <https://arxiv.org/abs/2602.11591>.
- [COT24] K. Coulembier, V. Ostrik, and D. Tubbenhauer. Growth rates of the number of indecomposable summands in tensor powers. *Algebr. Represent. Theory*, 27(2):1033–1062, 2024. URL: <https://arxiv.org/abs/2301.00885>, doi:10.1007/s10468-023-10245-7.
- [Cze24] A. Czenky. Unoriented 2-dimensional TQFTs and the category $\text{Rep}(S_t \wr \mathbb{Z}_2)$. *Quantum Topol.*, published online first, 2024. <https://arxiv.org/abs/2306.08826>, doi:10.4171/QT/221.
- [CKQW25] A. Czenky, J. Kesten, A. Quinonez, and C. Walton. On extended Frobenius structures. *Theory Appl. Categ.*, 44:1218–1269, 2025. <https://arxiv.org/abs/2410.18232>.
- [DGS25] P. Dłotko, D. Gurnari, and R. Sazdanovic. Data driven perspectives on knot theory. 2025. <https://arxiv.org/abs/2503.15103>.

- [ETW18] M. Ehrig, D. Tubbenhauer, and P. Wedrich. Functoriality of colored link homologies. *Proc. Lond. Math. Soc. (3)*, 117(5):996–1040, 2018. <https://arxiv.org/abs/1703.06691>, doi:10.1112/plms.12154.
- [EKM18] J. A. Ellis-Monaghan, L. H. Kauffman, and I. Moffatt. Edge colourings and topological graph polynomials. *Australas. J. Combin.*, 72(2):290–305, 2018. <https://arxiv.org/abs/1807.07500>.
- [EMM13] J. A. Ellis-Monaghan and I. Moffatt. A Penrose polynomial for embedded graphs. *European J. Combin.*, 34(2):424–445, 2013. <https://arxiv.org/abs/1106.5279>, doi:10.1016/j.ejc.2012.06.009.
- [GRY24] L. Gagnon-Ririe and M. B. Young. Frobenius–Schur indicators for twisted Real representation theory and two dimensional unoriented topological field theory. *J. Geom. Phys.*, 203:105260, 2024. <https://arxiv.org/abs/2310.03566>, doi:10.1016/j.geomphys.2024.105260.
- [Gre51] J.A. Green. On the structure of semigroups. *Ann. of Math. (2)*, 54:163–172, 1951. doi:10.2307/1969317.
- [HGR05] L. Helme-Guizon and Y. Rong. A categorification for the chromatic polynomial. *Algebr. Geom. Topol.*, 5:1365–1388, 2005. <https://arxiv.org/abs/math/0412264>, doi:10.2140/agt.2005.5.1365.
- [Jac04] M. Jacobsson. An invariant of link cobordisms from Khovanov homology. *Algebr. Geom. Topol.*, 4:1211–1251, 2004. <https://arxiv.org/abs/math/0206303>, doi:10.2140/agt.2004.4.1211.
- [Jae90] F. Jaeger. On transition polynomials of 4-regular graphs. In *Cycles and rays*, volume 301 of *NATO Adv. Sci. Inst. Ser. C Math. Phys. Sci.*, pages 123–150. Kluwer Acad. Publ., Dordrecht, 1990. doi:10.1007/978-94-009-0517-7_12.
- [JR06] E. F. Jasso-Hernandez and Y. Rong. A categorification for the Tutte polynomial. *Algebr. Geom. Topol.*, 6:2031–2049, 2006. <https://arxiv.org/abs/math/0512613>, doi:10.2140/agt.2006.6.2031.
- [Kau25] L. H. Kauffman. Categorification of chromatic, dichromatic and Penrose polynomials. Preprint, 2025. <https://arxiv.org/abs/2512.21027>, doi:10.48550/arXiv.2512.21027.
- [Kau87] L. H. Kauffman. State models and the Jones polynomial. *Topology*, 26(3):395–407, 1987. doi:10.1016/0040-9383(87)90009-7.
- [KLTVZ25] T. Kelomäki, A. Lacabanne, D. Tubbenhauer, P. Vaz, and V.L. Zhang. On detection probabilities of link invariants. 2025. <https://arxiv.org/abs/2509.05574>, doi:10.48550/arXiv.2509.05574.
- [Kho00] M. Khovanov. A categorification of the Jones polynomial. *Duke Math. J.*, 101(3):359–426, 2000. <https://arxiv.org/abs/math/9908171>, doi:10.1215/S0012-7094-00-10131-7.
- [KR21] M. Khovanov and L.-H. Robert. Foam evaluation and Kronheimer–Mrowka theories. *Adv. Math.*, 376:Paper No. 107433, 59, 2021. <https://arxiv.org/abs/1808.09662>, doi:10.1016/j.aim.2020.107433.
- [KST24] M. Khovanov, M. Sitaraman, and D. Tubbenhauer. Monoidal categories, representation gap and cryptography. *Trans. Amer. Math. Soc. Ser. B*, 11:329–395, 2024. URL: <https://arxiv.org/abs/2201.01805>, doi:10.1090/btran/151.
- [Koc04] J. Kock. *Frobenius algebras and 2D topological quantum field theories*, volume 59 of *London Mathematical Society Student Texts*. Cambridge University Press, Cambridge, 2004. doi:10.1017/CB09780511615443.
- [KM19] P. B. Kronheimer and T. S. Mrowka. Tait colorings, and an instanton homology for webs and foams. *J. Eur. Math. Soc. (JEMS)*, 21(1):55–119, 2019. <https://arxiv.org/abs/1508.07205>, doi:10.4171/JEMS/831.
- [LZ04] S. K. Lando and A. K. Zvonkin. *Graphs on surfaces and their applications*. Encyclopaedia of Mathematical Sciences, volume 141. Springer, Berlin, 2004. doi:10.1007/978-3-540-38361-1.
- [LM08] M. Loebl and I. Moffatt. The chromatic polynomial of fatgraphs and its categorification. *Adv. Math.*, 217(4):1558–1587, 2008. <https://arxiv.org/abs/math/0511557>, doi:10.1016/j.aim.2007.11.016.

- [LR11] K. Luse and Y. Rong. A categorification for the Penrose polynomial. *J. Knot Theory Ramifications*, 20(1):141–157, 2011. doi:10.1142/S021821651100867X.
- [Man07] V. O. Manturov. Khovanov homology for virtual knots with arbitrary coefficients. *J. Knot Theory Ramifications*, 16(3):345–377, 2007. <https://arxiv.org/abs/math/0601152>, doi:10.1142/S0218216507005336.
- [MPS17] S. Morrison, E. Peters, and N. Snyder. Categories generated by a trivalent vertex. *Selecta Math. (N.S.)*, 23(2):817–868, 2017. URL: <https://arxiv.org/abs/1501.06869>, doi:10.1007/s00029-016-0240-3.
- [Pen71] R. Penrose. Applications of negative dimensional tensors. In D. J. A. Welsh, editor, *Combinatorial Mathematics and its Applications*, pages 221–244. Academic Press, New York, 1971.
- [Tag13] K. Tagami. A Khovanov type invariant derived from an unoriented HQFT for links in thickened surfaces. *Internat. J. Math.*, 24(10):1350078, 28, 2013. URL: <https://arxiv.org/abs/1311.1909>, doi:10.1142/S0129167X1350078X.
- [TL71] H.N.V. Temperley and E.H. Lieb. Relations between the “percolation” and “colouring” problem and other graph-theoretical problems associated with regular planar lattices: some exact results for the “percolation” problem. *Proc. Roy. Soc. London Ser. A*, 322(1549):251–280, 1971. doi:10.1098/rspa.1971.0067.
- [Tub24a] D. Tubbenhauer. On rank one 2-representations of web categories. *Algebr. Comb.* 7 (2024), no. 6, 1813–1843 <https://arxiv.org/abs/2307.00785>, doi:10.5802/alco.389.
- [Tub25] D. Tubbenhauer. Quantum topology without topology. 2025. <https://arxiv.org/abs/2506.18918>.
- [Tub24b] D. Tubbenhauer. Sandwich cellularity and a version of cell theory. *Rocky Mountain J. Math.*, 54(6):1733–1773, 2024. <https://arxiv.org/abs/2206.06678>, doi:10.1216/rmj.2024.54.1733.
- [Tub14] D. Tubbenhauer. Virtual Khovanov homology using cobordisms. *J. Knot Theory Ramifications*, 23(9):1450046, 91, 2014. <https://arxiv.org/abs/1111.0609>, doi:10.1142/S0218216514500461.
- [TZ25] D. Tubbenhauer and V. Zhang. Big data comparison of quantum invariants. 2025. To appear in *Journal of Experimental Mathematics*. <https://arxiv.org/abs/2503.15810>.
- [TT06] V. Turaev and P. Turner. Unoriented topological quantum field theory and link homology. *Algebr. Geom. Topol.*, 6:1069–1093, 2006. <https://arxiv.org/abs/math/0506229>, doi:10.2140/agt.2006.6.1069.
- [TV17] V.G. Turaev and A. Virelizier. *Monoidal categories and topological field theory*, volume 322 of *Progress in Mathematics*. Birkhäuser/Springer, Cham, 2017. doi:10.1007/978-3-319-49834-8.
- [Yam89] S. Yamada. An invariant of spatial graphs. *J. Graph Theory*, 13(5):537–551, 1989. doi:10.1002/jgt.3190130503.

D.W.C.: THE UNIVERSITY OF SYDNEY, SCHOOL OF MATHEMATICS AND STATISTICS F07, NSW 2006, AUSTRALIA
Email address: daniel.collison@sydney.edu.au

D.T.: THE UNIVERSITY OF SYDNEY, SCHOOL OF MATHEMATICS AND STATISTICS F07, OFFICE CARSLAW 827,
 NSW 2006, AUSTRALIA, WWW.DTUBBENHAUER.COM, [HTTPS://ORCID.ORG/0000-0001-7265-5047](https://ORCID.ORG/0000-0001-7265-5047)
Email address: daniel.tubbenhauer@sydney.edu.au